Chapter 7
Design for Vibration

The body structure is a resonant system with an infinite number of natural frequencies. If any of these resonances occur at the wrong frequency, objectionable or destructive levels of vibration will result. In this chapter, we will investigate ways to avoid this and identify desirable vibration behavior for the body structure. We will do this from a design perspective—where shall we place these body structure resonances to result in satisfactory vibration performance?

7.1 First-Order Vibration Modeling

Generally during the early design stages we are not interested in estimating the *precise* vibration amplitudes. We wish only to assure that the amplitude will not be objectionably large to the *receiver* of the vibration. We can do this by assuming, for a well-designed vehicle, that the frequency of the vibration *source* does not coincide with a resonance in the vibration *path* (i.e., the vibration is uncoupled). This assumption will allow us to simplify our analysis models by considering the well-designed automobile to be a set of *independent* single-degree-of-freedom oscillators in which the natural frequencies of these oscillators do not coincide. Following is an example of this concept.

Example: First-order vibration model of steering column

In this example, we look at a vibration system consisting of the powertrain, steering column, and driver air cushion restraint, Figure 7.1. The steering column mounting structure, Figure 7.2a, is designed to meet static stiffness requirements—in this case, a vertical stiffness of *200 N/mm* as measured at the steering wheel. This level of stiffness provides a very small static downward deflection (*1 mm*) under a downward load (*200 N*), which the driver may impart to the steering wheel. This deflection is perceived by the driver as a "solid" feel. The steering wheel, mass *m=5 kg*, is mounted on this column structure, and the combination behaves as a single-degree-of-freedom oscillator, Figure 7.2b. The natural frequency of this oscillator is given by (this relationship will be developed in Section 7.3) [1]:

$$\omega_n = \sqrt{\frac{k}{m}}$$

where:

ω_n = Natural frequency in radians /sec

k = Stiffness

m = Mass

For this example, *k=200 N/mm, m=5 kg* and

$$\omega_n = \sqrt{\frac{k}{m}} = \sqrt{\frac{(200N/mm)(1000mm/meter)}{5kg}}$$

$$\omega_n = \sqrt{40000N/meter\,kg} = 200rad/\sec$$

Note units: $1\ N = 1\ kg\ m/_{s}^{2}$

It is often convenient to express the frequency in *Hz* (cycles/sec):

$$f_n(Hz) = \omega(rad/s)(1cycle/2\pi\,rad)$$

$$f_n = 31.8Hz$$

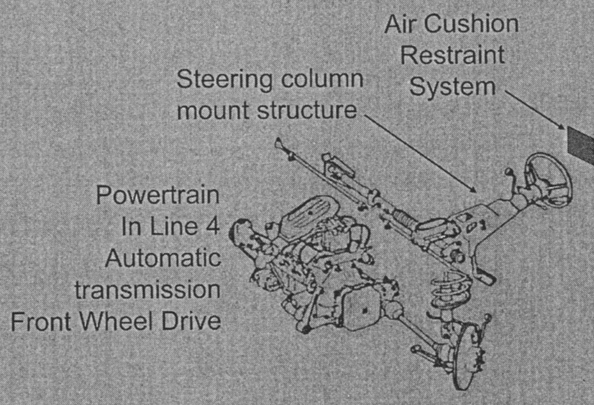

Figure 7.1 Vibration interaction example.

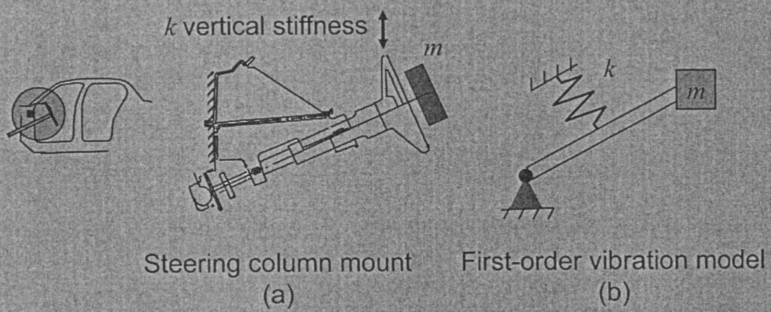

Figure 7.2 Steering column resonant system.

The "goodness" of this resonant frequency depends on whether it coincides with a forcing frequency (source), and also depends on how the driver (receiver) perceives a vibration at this frequency at his hands.

Example: First-order model of vibration source

Consider a source of vibration which may excite the steering column—a four-cylinder engine in a transverse front-wheel-drive configuration with an automatic transmission. Each time a cylinder fires, a torque pulse occurs at the crankshaft, Figure 7.3. For a four-stroke engine, this pulse occurs once every two revolutions for each cylinder. With four cylinders and an engine speed of N revolutions per minute, this torque pulse excitation occurs at a frequency of

$$\Omega = (4\,cylinders)(1\,pulse/2\,rev)(N\,rev/\mathrm{min})(1\,\mathrm{min}/60\,\mathrm{sec})$$
$$\Omega = (N/30)\,Hz$$

where:
Ω = Torque pulse excitation frequency (Hz)

N = Engine rotational speed (rev/min)

When such a powertrain is at idle speed *N=700 rev/min* with the transmission in Drive, these torque pulses are reacted by the engine block. The torque pulse frequency for this example is *N=700 rev/min* and $\Omega = 700/30 = 23.3$ *Hz*.

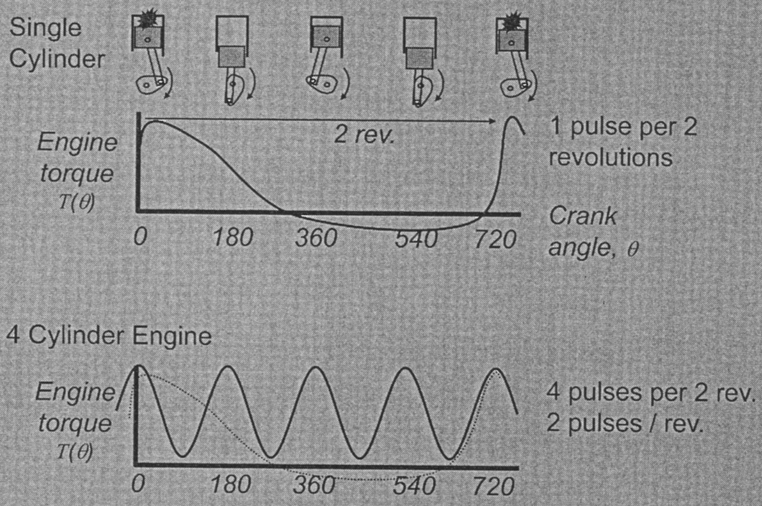

Figure 7.3 Engine torque variation.

This idle condition imposes an oscillating input from the block through the engine mounts, into the body, and ultimately to the steering column mount. However, since the forcing frequency of the torque pulses, $\Omega = 23.3$ *Hz*, does not coincide with the resonant frequency of the steering column, $fn = 31.8$ *Hz*, we would not expect a troublesome vibration amplitude.

Example: Coupled resonance

Now consider that a driver side *Air Cushion Restraint System*, ACRS, is mounted on the steering wheel, Figure 7.1. The ACRS adds an additional mass, *4.5 kg*, to the resonant model of the previous example. The steering column resonant frequency now changes:

$$\omega_n = \sqrt{\frac{k}{m}} = \sqrt{\frac{(200N/mm)(1000mm/meter)}{(5+4.5)kg}}$$

$$\omega_n = \sqrt{21053N/meter\,kg} = 145rad/\sec$$

$$f(Hz) = 145(rad/s)(1cycle/2\pi\,rad)$$

$$f = 23.1Hz$$

Now the engine torque pulse excitation frequency approximately coincides with the steering column resonance, Figure 7.4. This undesirable condition will result in large steering column vibration levels which will be perceived by the customer, Figure 7.5. It is this condition—coinciding source and path frequencies—which we attempt to avoid during design.

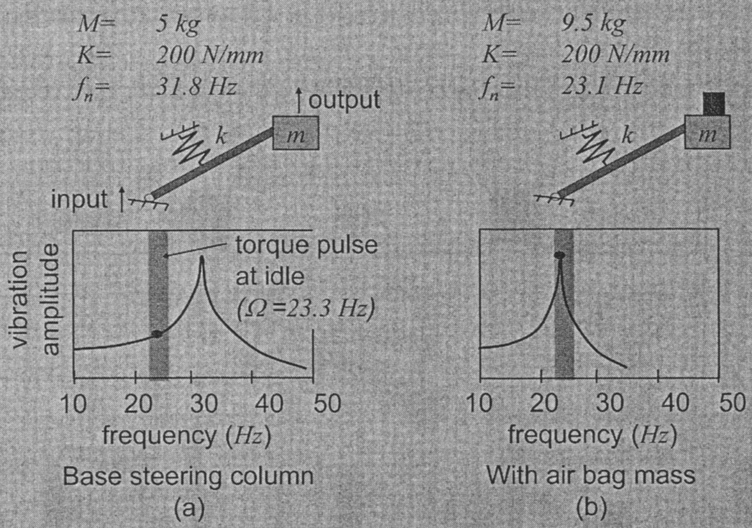

Figure 7.4 Source-path interaction.

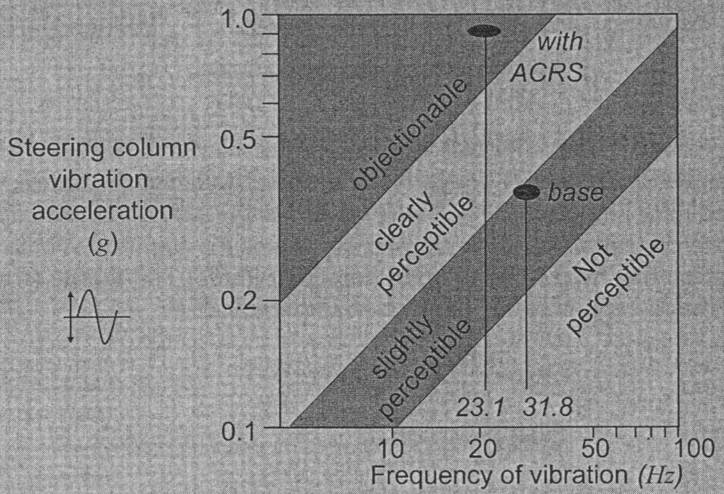

Figure 7.5 Driver tactile perception.

(Note that the addition of the ACRS did not cause any difficulties with the *static* behavior of the steering column/ACRS system; there would be no excessive static deflection with the ACRS installed, nor would the strength of the column mount be exceeded by the addition of the ACRS. It is only when we look at the vehicle system—including the source of vibration energy—that we find this problem.)

7.2 Source-Path-Receiver Model of Vibration Systems

The example of Section 7.1 suggests a way to view vibratory systems for design purposes. The system, Figure 7.6, is viewed as consisting of:

1. A *Source* of vibration energy (engine torque pulses in Section 7.1 example)
2. A *Path* for the vibration consisting of a series of subsystems (the steering column with ACRS)
3. A *Receiver* which determines the acceptability of the vibration level (the driver's hands).

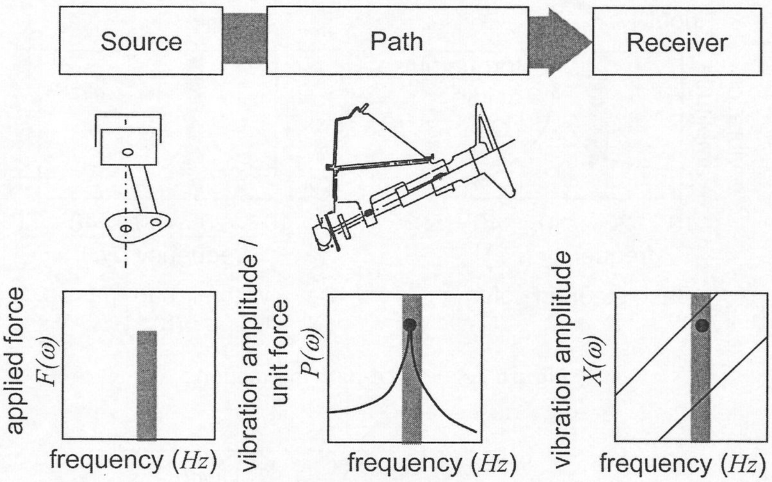

Figure 7.6 General vibration model.

The vibration characteristics for each of these entities may be viewed as a function of vibration frequency (frequency domain), Figure 7.6 bottom. For the source, we have a generalized force amplitude, $F(\omega)$, being applied to the system; for the path, we have a transfer function, $P(\omega)$. This transfer function is the amplitude of the output (deflection) resulting from a unit of input (force amplitude); and for the receiver, a relation for the perception of the vibration at amplitude $X(\omega)$:

$$F(\omega)\left[\frac{X(\omega)}{F(\omega)}\right] = X(\omega)$$

$$F(\omega)[P(\omega)] = X(\omega) \qquad (7.1a)$$

$$\uparrow \qquad\quad \uparrow \qquad\quad \uparrow$$

Source Path Sensed by Receiver

where:

$F(\omega)$ = Source amplitude

$X(\omega)$ = Response amplitude

$[P(\omega)]$ = Path transfer function [response, $X(\omega)$, per unit of input, $F(\omega)$]

In the above relationship, the path is viewed as a single subsystem which responds directly to the source. This model we used in the steering column example. In many cases in automobile design, the path is a series of subsystems: for example, a vibration force, $F(\omega)$, applied at the spindle of the front suspension. This applied force is attenuated by the suspension characteristics, $[T(\omega)]$, and a reduced force, $F_T(\omega)$, is transmitted to the body structure through the suspension attachments. This behavior can be described by the relationship,

$$F(\omega)\left[\left(\frac{F_T(\omega)}{F(\omega)}\right)\left(\frac{X(\omega)}{F_T(\omega)}\right)\right] = X(\omega)$$

$$F(\omega)[T(\omega)P(\omega)] = X(\omega) \tag{7.1b}$$

↑ Source ↑ Path ↑ Sensed by Receiver

where:

$F(\omega)$ = Source amplitude

$X(\omega)$ = Response amplitude

$T(\omega)$ = Isolation characteristic of a subsystem in the path (force transmitted, $F_T(\omega)$, per unit force applied, $F(\omega)$)

$F_T(\omega)$ = Force transmitted through a subsystem of the path

$P(\omega)$ = Body structure transfer function

Equation 7.1b will be used to develop design requirements for the body structure vibration performance. Later in this chapter we will look closely at the four vibration systems shown in the table below.

Table 7.1 Four automobile vibration systems.

Vibration System	Source $F(\omega)$	Isolator $T(\omega)$	Force into Body $F_T(\omega)$	Body Transfer Function $P(\omega)$	Body Deflection $X(\omega)$
1	Powertrain unbalance force	Mounted powertrain	Force through engine mounts	Body structure	Deflection at seat, steering column
2	Force at suspension spindle	Suspension	Force through shock absorber and ride spring	Body structure	Deflection at seat, steering column
3	Road deflection at tire patch	Suspension	Force through shock absorber and ride spring	Body structure	Deflection at seat, steering column
4	High frequency chassis deflections	Chassis links with end bushings	Body panel vibrations	Passenger compartment acoustic resonances	Interior sound pressure

7.2.1 Automobile vibration spectrum

As each of the vibration characteristics, *F(ω), T(ω), $F_t(\omega)$, P(ω), and X(ω),* depend on frequency, *ω*, it is useful to consider the vibration spectrum for an automobile, Figure 7.7. Below *10 Hz* the body structure acts as a rigid body. Above *100 Hz*, body vibration behavior is more localized and influenced by structural details. For these design details we have the ability to take corrective measures for poor performance later in the design sequence. We are most concerned with the frequency range of *10–100 Hz* in body structure design. Behavior of the structure within this range is that of the primary bending and torsion resonances. These are set by the overall body architecture which, once established, cannot easily be changed in the later design stages. Therefore it is important to design-in proper behavior for this range during the early stages of design.

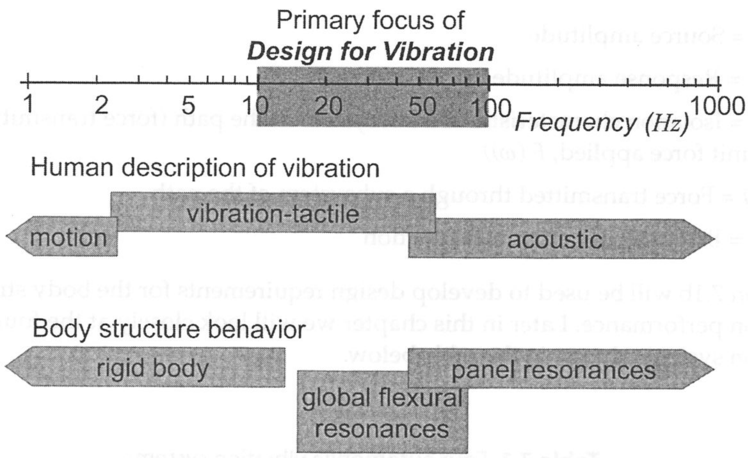

Figure 7.7 Vehicle vibration spectrum.

7.2.2 Human response to vibration

The objective of designing for vibration is to create an acceptable vibration environment for the automobile passengers. There are considerable data which relate human preference to vertical seat vibration level. In a typical test, a sinusoidal vibration level is imposed at a specific frequency to the seat and the subject is asked to subjectively describe the vibration—imperceptible, just perceptible, annoying. The data from these evaluations are plotted on a vibration amplitude vs. frequency plot as lines of constant comfort. A classical criterion is the Janeway curve, Figure 7.8, which describes the boundary of acceptable vibration amplitude [2]. Figure 7.9 is a summary of data from several contemporary sources compared with the Janeway curve [3, 4, 5]. The general character of all these iso-comfort curves is U shaped, with the area least tolerated occurring in the *6–20 Hz* range. These data give us some idea for acceptable vibration levels as we use the source-path-receiver model to design the structure for vibration behavior.

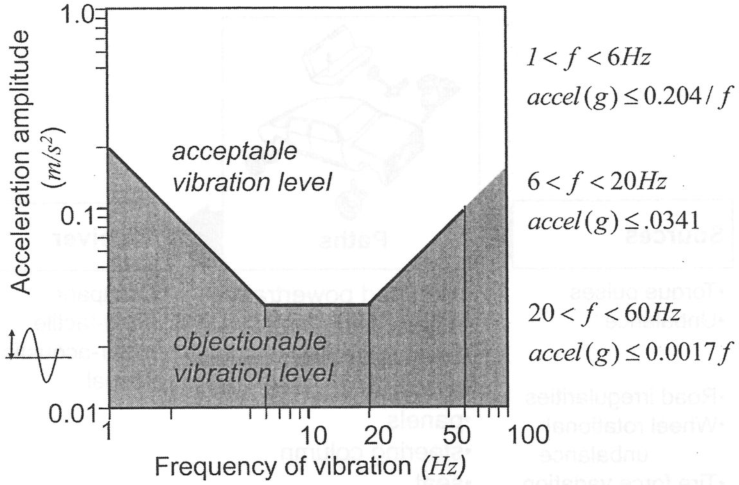

Figure 7.8 Janeway vertical seat vibration criteria.

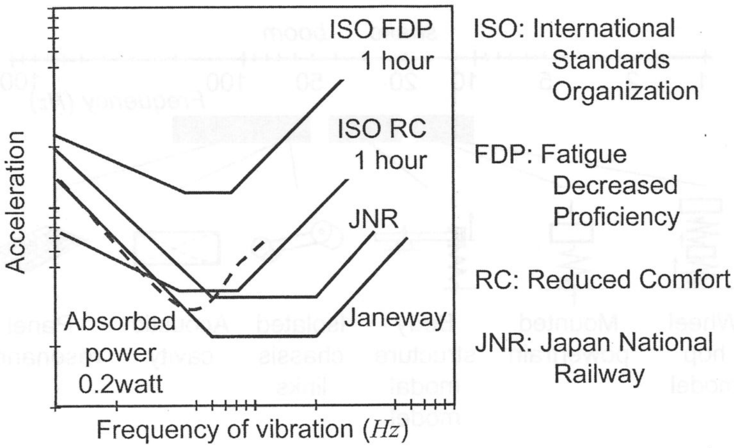

Figure 7.9 Comparison of recommended vibration limits. (Courtesy of SAE International)

In the following sections we will look at some important vibration systems of the automobile using this source-path-receiver model of Equation 7.1b, Figure 7.10. We shall model the isolation behavior, $T(\omega)$, and also the body structure transfer function, $P(\omega)$, as single-degree-of-freedom (SDOF) oscillators, Figure 7.11. Therefore in the next section, we will begin by developing the equations of motion for a general SDOF system.

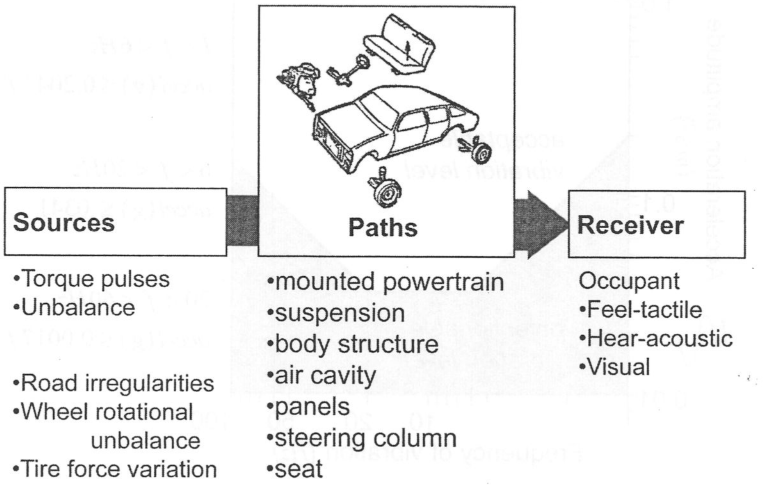

Figure 7.10 Automobile vibration model.

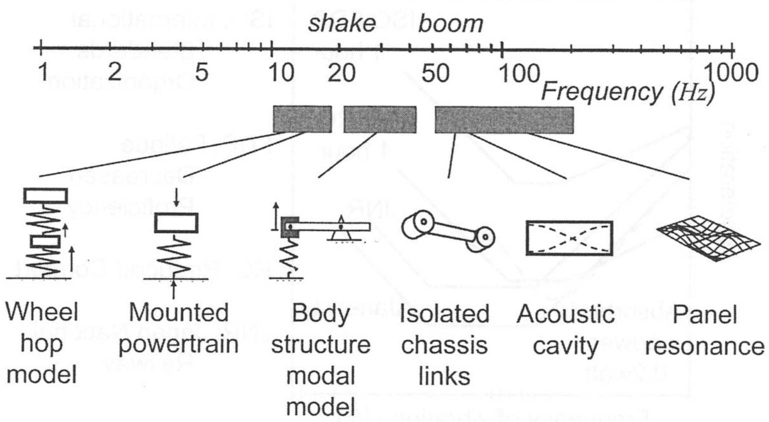

Figure 7.11 Major vibratory systems.

7.3 Frequency Response of a Single-Degree-of-Freedom System

As an example of a SDOF system, consider the vertical motion of a powertrain mounted on engine mounts, Figure 7.12a. (In a SDOF system, only one coordinate is needed to describe the motion. This coordinate may be either a linear or rotational deflection.) We assume the powertrain is mounted to ground and that a vertical sinusoidal force is applied with amplitude F and frequency ω. With a sinusoidal forcing function, the vertical displacement will also be sinusoidal with amplitude X and frequency ω:

$$\begin{aligned} f(t) &= F\sin(\omega t) \\ x(t) &= X\sin(\omega t) \end{aligned} \tag{7.2}$$

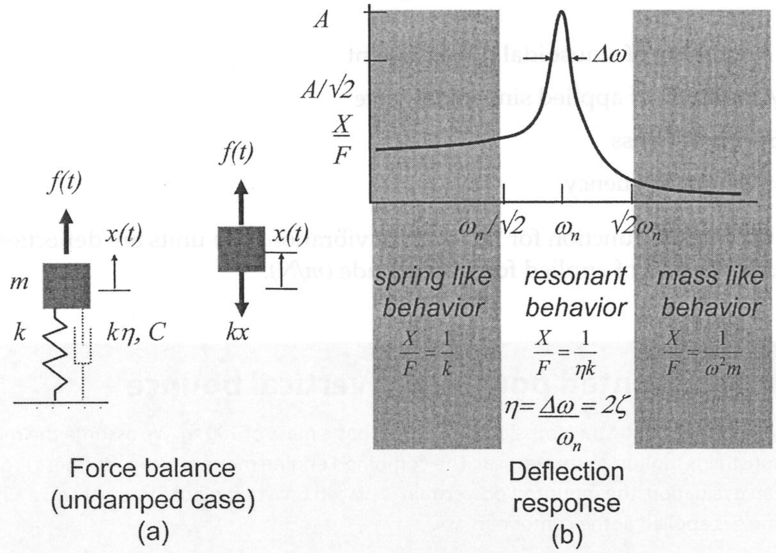

Figure 7.12 Single-degree-of-freedom system behavior.

7.3.1 Equation of motion for SDOF system

Consider a free body of the mass, Figure 7.12a, with a positive deflection of x [6]:

$$\Sigma(\text{forces acting on m}) = m\frac{d^2x(t)}{dt^2}$$

$$f(t) - kx(t) = m\frac{d^2x(t)}{dt^2} \qquad (7.3)$$

$$\frac{d^2x(t)}{dt^2} = -X\omega^2\sin(\omega t)$$

$$F\sin(\omega t) = kX\sin(\omega t) - mX\omega^2\sin(\omega t) \qquad (7.4)$$

$$F = kX - m\omega^2 X$$

$$\frac{X}{F} = \frac{1}{k - m\omega^2}$$

When $\omega^2 = k/m$, the denominator of this expression goes to zero and we have very large deflections. This frequency is the natural or resonant frequency for this system:

$$\omega_n^{\ 2} = \frac{k}{m} \qquad (7.5)$$

With this definition the response, $P(\omega)$, is:

$$\frac{X}{F} = \frac{1/k}{1-\left(\frac{\omega}{\omega_n}\right)^2} = P(\omega) \qquad (7.6)$$

where:

X = Amplitude of sinusoidal displacement

F = Amplitude of applied sinusoidal force

k = Spring stiffness

ω_n = Natural frequency

This is the transfer function for this path of vibration. The units are deflection amplitude per unit of applied force amplitude *(m/N)*.

Example: Mounted powertrain vertical bounce

A four-cylinder, automatic transmission powertrain has a mass of *100 kg*. We assume the mount system constrains motion to the vertical. The combined engine mount vertical stiffness is *600 N/mm*. For an evaluation, the mounted powertrain is placed on a bed plate (ground) and a sinusoidal vertical force is applied at the center of mass.

a) Determine the natural frequency for this bounce mode

$$\omega_n^2 = \frac{k}{m}$$

$$\omega_n^2 = \frac{(600N/mm)(1000mm/m)}{100kg} = 6000N/kg \ \left[(\text{kg m}/\text{s}^2)/\text{kg}\right]$$

$$\omega_n = 77.46 rad/\sec$$

$$f_n = 38.73 rad/\sec(cycle/2\pi rad) = 12.33 Hz$$

b) At a certain engine speed, the reciprocating masses in the engine apply a vertical sinusoidal force of amplitude of *500 N* at a frequency of *15 Hz*; what is the deflection amplitude of the powertrain?

$$\frac{X}{F} = \frac{1/k}{1-\left(\dfrac{\omega}{\omega_n}\right)^2} = \frac{1/(6x10^5 N/m)}{1-\left(\dfrac{\omega}{77.46 rad/s}\right)^2} = \frac{1.67x10^{-6}}{1-\left(\dfrac{\omega}{77.46 rad/s}\right)^2} m/N$$

$$\frac{X}{F} = \frac{1.67x10^{-6}}{1-\left(\dfrac{(15cycle/s)(2\pi rad/cycle)}{77.46 rad/s}\right)^2} m/N = -3.48x10^{-6} m/N$$

$$X = (-3.48x10^{-6} m/N)(500N) = -1.738x10^{-3} m$$

Note, the negative sign for X means that the deflection and force sinusoids are out of phase by *180°*. Note also that this dynamic deflection is greater than if the force had been applied statically: *500 N/(600 N/mm)=0.833x10⁻³ m*.

7.3.2 Relation of vibration amplitudes

To gain insight into SDOF systems under sinusoidal motion, consider the relationship between the amplitudes for displacement, *x(t)*, velocity, *v(t)*, and acceleration, *a(t)*. Given a displacement amplitude, *X*:

$$\begin{aligned} displacement &= x(t) = X\sin(\omega t) \\ velocity &= \frac{dx(t)}{dt} = X\omega\cos(\omega t) \\ acceleration &= \frac{d^2x(t)}{dt^2} = -X\omega^2\sin(\omega t) \end{aligned} \tag{7.7}$$

So for any frequency, ω, these amplitudes are related as

$$\begin{aligned} displacement\ amplitude &= X \\ velocity\ amplitude &= X\omega \\ acceleration\ amplitude &= X\omega^2 \end{aligned} \tag{7.8}$$

Often in vibration testing, an accelerometer is used to measure vibration amplitude. The relations above can be used to convert between amplitudes.

Example: Powertrain vibration test

An accelerometer is applied to a powertrain under test. During a vibration test at a sinusoidal forcing frequency of *40 Hz*, the amplitude recorded by the accelerometer is *10 g*. What is the deflection amplitude?

$$\begin{aligned} &acceleration\ amplitude = X\omega^2 \\ &X = acceleration\ amplitude / \omega^2 \\ &X = (10g)(9.8m/s^2)/\left[40Hz(2\pi rad/cycle)\right]^2 \\ &X = 1.55x10^{-3}m \end{aligned}$$

7.3.3 Regions of vibration behavior

Plotting Equation 7.6 for $P(\omega)$ against frequency, we can identify three important regions, Figure 7.12b; at frequencies much below the resonance frequency, $(\omega << \omega_n)$ we have spring-like behavior:

$$\begin{aligned} F &= kX \\ \left|\frac{X}{F}\right| &= \frac{1}{k} \end{aligned} \tag{7.9}$$

For frequencies much higher than the resonance frequency, $(\omega >> \omega_n)$, we have mass-like behavior:

$$\begin{aligned} F &= m(acceleration) \\ F &= m(-X\omega^2) \\ \left|\frac{X}{F}\right| &= \frac{1}{\omega^2 m} \end{aligned} \tag{7.10}$$

At resonance, $(\omega = \omega_n)$, the vibration amplitude grows very large—infinite in this undamped model. For real systems, the vibration amplitude at resonance is large, but is limited by damping.

7.3.4 Amplitude at resonance

For behavior close to the resonant frequency, the deflection of the system is limited only by damping forces, which dissipate vibration energy. A common damping model is *viscous damping*, where the damping force is proportional to, and in phase with, velocity.

$$F_D = C(velocity) \tag{7.11}$$

where C = Viscous damping coefficient

Often, the damping coefficient is expressed in terms of the viscous damping factor, ζ:

$$\zeta = \frac{C}{2\sqrt{km}} \tag{7.12}$$

For this case, the amplitude at resonance is given by:

$$\begin{aligned}
&F_D = C(velocity)\\
&|F_D| = C(X\omega) = 2\zeta\sqrt{km}(X\omega) = 2\zeta k\sqrt{m/k}(X\omega)\\
&\left|\frac{X}{F_D}\right| = \frac{1}{2\zeta k(\omega/\omega_n)}\\
&at\ resonance\ \omega = \omega_n\\
&\left|\frac{X}{F_D}\right|_{\omega=\omega_n} = \frac{1}{2\zeta k}
\end{aligned} \tag{7.13}$$

Viscous damping is generally assumed for suspension shock absorbers where a typical value for damping factor, C, is approximately *C=2 Nsec/mm (11 lb sec/in).*

A second type of damping is *structural damping*, in which the damping force is proportional to deflection, X, but in phase with velocity. The structural damping factor, η, describes the damping force as a fraction of force through the stiffness element:

$$|F_D| = (\eta k X) \tag{7.14}$$

As with viscous damping, the damping force determines the amplitude at resonance:

$$\left|\frac{X}{F_D}\right|_{\omega=\omega_n} = \frac{1}{\eta k} \tag{7.15}$$

Structural damping is typically used to describe the behavior of metal structures. While structural damping for the base metal is typically quite low *($0.0001<\eta<0.001$)*, significant damping occurs in built-up metal structures at the welded joints. For a spot-welded automobile body, the damping factor is on the order of *($0.03<\eta<0.1$)* [7].

(The same mathematical form is also used to characterize damping behavior of elastomeric mounts [8]. In that case the factor η is called the loss factor, having a typical range from $0.05<\eta<0.2$.)

Comparing Equations 7.13 and 7.15, note the relation of viscous damping and structural damping at the resonant frequency:

$$\eta = 2\zeta \tag{7.16}$$

For either viscous or structural damping, the damping coefficient may be estimated by the bandwidth at the half-power amplitude, as shown in Figure 7.12b:

$$\eta = \frac{\Delta\omega}{\omega_n} \tag{7.17}$$

where $\Delta\omega$ is the bandwidth measured at the half-power amplitude [√2(amplitude at resonance)], Figure 7.12b.

Example: Powertrain vibration amplitude at resonance

A powertrain has a mass of *100 kg*. The engine mount system constrains motion to the vertical. The combined engine mount vertical stiffness is *600 N/mm* with a damping ratio of $\eta=0.1$. An oscillating force of *500 N* is applied at the resonance frequency of the system. What is the deflection amplitude?

$$\left|\frac{X}{F_D}\right|_{\omega=\omega_n} = \frac{1}{\eta k}$$

$$\left|\frac{X}{F_D}\right|_{\omega=\omega_n} = \frac{1}{(.1)(600N/mm)(1000mm/m)} = 0.0167x10^{-3}m/N$$

$$X = 500N(0.0167x10^{-3}m/N) = 8.33x10^{-3}m$$

7.3.5 Transfer function as log-log plot

Because the source-path-receiver model, Equation 7.1b, involves multiplying frequency characteristics, it is helpful to display $F(\omega)$, $T(\omega)$, $P(\omega)$, and $X(\omega)$ as log-log graphs. When displayed in this way, the multiplication in Equation 7.1b is visualized by adding the y values of the response plots. For example, the response of a SDOF system, Equation 7.6, is plotted on logarithmic axes in Figure 7.13.

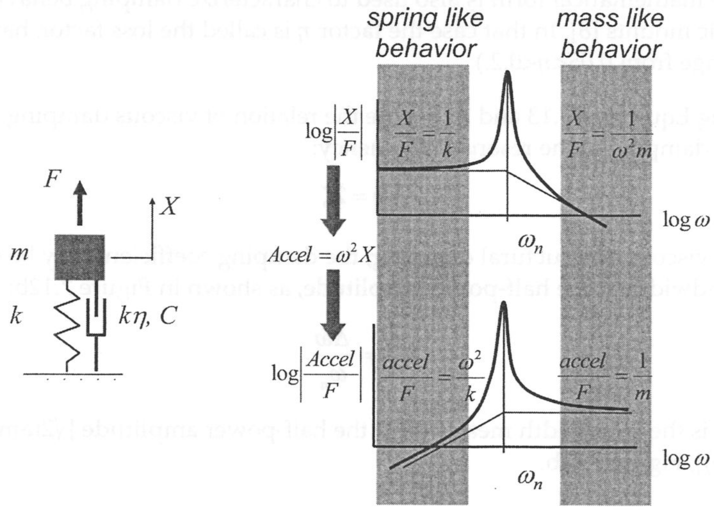

Figure 7.13 Log displacement output vs. acceleration output.

7.4 SDOF Models of Vehicle Vibration Systems

With the background of Section 7.3, we can now look at some specific vehicle systems using the model of Equation 7.1b.

$$F(\omega)\left[\left(\frac{F_T(\omega)}{F(\omega)}\right)\left(\frac{X(\omega)}{F_T(\omega)}\right)\right]=X(\omega)$$

$$F(\omega)[T(\omega)P(\omega)]=X(\omega) \qquad \text{(7.1b) repeated}$$

$$\uparrow \qquad \uparrow \qquad \uparrow$$

Source Path Sensed by Receiver

In each case, we are interested in how the forces being applied to the body structure, F_T, vary with frequency, Figure 7.14. Understanding this, we can then decide where the structural resonances of the body should be placed.

7.4.1 Powertrain path: Reciprocating unbalance

The first system we will look at is the Powertrain path, Table 7.2, Figure 7.15.

Table 7.2 Powertrain path vibration system.

Source F(ω)	Isolator T(ω)	Force into Body $F_T(\omega)$	Body Structure Transfer Function P(ω)	Body Deflection X(ω)
Powertrain unbalance force	Mounted powertrain	Force through engine mounts	Body structure	Deflection at seat, steering column

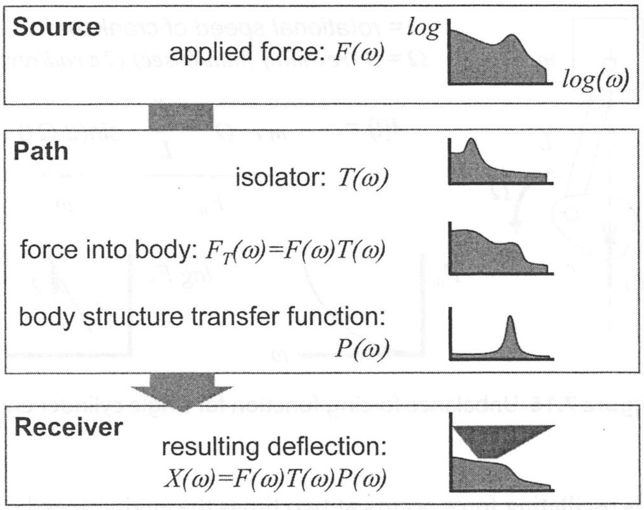

Figure 7.14 Characterizing behavior with frequency response.

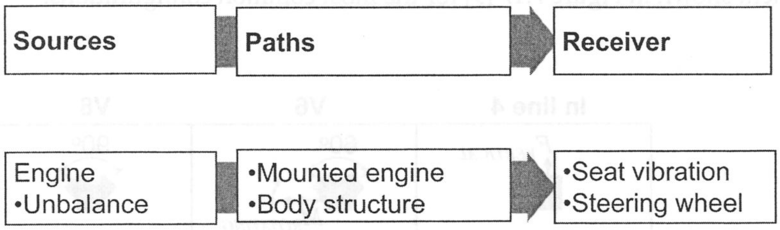

Figure 7.15 Powertrain-driven vibration.

The reciprocating elements of the engine—piston and connecting rod—impose forces on the crankshaft, Figure 7.16. For each cylinder, the oscillating forces are given by [9]:

$$\begin{aligned} f(t) &= \left[mr\Omega^2 \frac{r}{l} \right] \sin(2\Omega t) \\ f(t) &= \qquad F \qquad \sin(\omega t) \end{aligned} \tag{7.18}$$

where:

$f(t)$ = Oscillating force applied to the crankshaft

m = Reciprocating mass

r = Crank shaft offset shown in Figure 7.16

l = Connecting rod length

Ω = Engine speed in rad/s [$\Omega = N\ (rpm)\ (2\pi\ rad/rev)(1\ min/60\ sec)$]

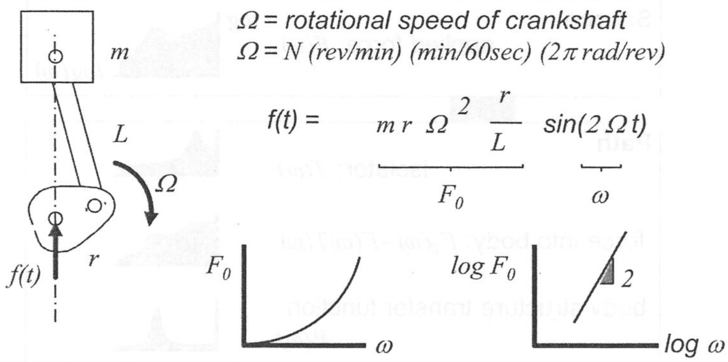

Figure 7.16 Unbalance forcing function for single cylinder engine.

Note that this oscillating force occurs at two times the engine speed due to the kinematics of the piston motion, and that the amplitude increases with the square of the engine speed. For engines with multiple cylinder configurations—L4, V6, V8—the unbalance forces of the individual cylinders combine to the resultant force or moment shown in Figure 7.17 [9] for the most common configurations.

	In line 4	V6	V8
	$F_{VERTICAL}$ planar crankshaft	60° $M_{ROTATING}$ even 120° crankshaft	90° even 90° crankshaft
Excitation amplitude (2 x engine speed)	$F_{VERTICAL} = 4mr\frac{r}{l}\Omega^2$	$M_{ROT} = \frac{3}{2}mr\frac{r}{l}\Omega^2 a$ cylinder spacing a	*None*
Balance strategy	$F_{VERTICAL}$ may be eliminated with dual counter rotating balance shafts at 2 x engine speed	crankshaft counter weights balance the primary rotating couple leaving the above moment	crankshaft counter weights balance the primary rotating couple

Figure 7.17 Unbalance forcing function for multiple cylinder engines.

With the source-path-receiver model shown in Figure 7.15, we have engine unbalance forces applied to the powertrain. The path into the body is through the mounted powertrain acting as an isolator. For body design, we are interested in the force transmitted through the engine mounts into the body structure. The mounted powertrain is a SDOF system, Figure 7.18, with frequency response given by Equation 7.4. The transmitted force though the engine mounts is then:

$$\begin{aligned} F_T &= kX \\ \frac{X}{F} &= \frac{1/k}{1-\left(\dfrac{\omega}{\omega_n}\right)^2} \\ \frac{Xk}{F} &= \frac{1}{1-\left(\dfrac{\omega}{\omega_n}\right)^2} \\ \frac{F_T}{F} &= \frac{1}{1-\left(\dfrac{\omega}{\omega_n}\right)^2} = T(\omega) \end{aligned} \tag{7.19}$$

where:

F_T = Force transmitted to body through engine mounts

F = Force applied to powertrain

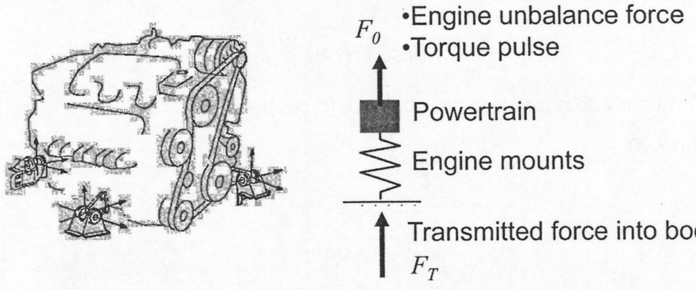

Figure 7.18 First order model for powertrain on rigid base.

In this expression, F is the magnitude of the unbalance force, and F_T is the force applied to the body structure through the engine mounts. When the magnitude of (F_T/F) is greater than one, the engine mount system is amplifying the unbalance forces; when it is less than one, it is reducing—isolating—the unbalance forces. This isolation begins to occur when:

$$\frac{F_T}{F} = abs\left[\frac{1}{1-\left(\frac{\omega}{\omega_n}\right)^2}\right] < 1$$

$$\pm 1 < 1-\left(\frac{\omega}{\omega_n}\right)^2$$

$$2 < \left(\frac{\omega}{\omega_n}\right)^2 \tag{7.20}$$

$$\sqrt{2} < \frac{\omega}{\omega_n}$$

$$\omega > \omega_n\sqrt{2}$$

Example: Isolation frequency of a mounted powertrain

A four-cylinder, automatic-transmission powertrain has a mass of *100 kg*. The engine mount system constrains motion to the vertical. The combined engine mount vertical stiffness is *600 N/mm*. For an evaluation, the mounted powertrain is placed on a bed plate (ground) and a sinusoidal vertical force is applied to the center of mass.

a) Determine the bounce natural frequency; in the example of Section 7.3 we found that

$$\omega_n = 77.46\,rad/\sec$$
$$f_n = 38.73\,rad/\sec(cycle/2\pi rad) = 12.33\,Hz$$

b) At what frequency does isolation of unbalance forces begin?

From Equation 7.20:

$$\omega > \omega_n\sqrt{2}$$
$$\omega > 77.46\sqrt{2}$$
$$\omega > 109.54\,rad/s$$
$$f_n = 17.43\,Hz$$

c) What is the engine speed at which isolation begins?

The unbalance forces occur at two times the engine speed, Equation 7.18:

$$\omega = 2\Omega$$
$$\Omega = (109.54\,rad/s)/2 = 54.77\,rad/s$$
$$or$$
$$N = 54.77\,rad/s(1rev/2\pi rad)(60s/\min) = 523\,RPM$$

The equation above is for an undamped system. If we consider engine mounts with loss factor η, we replace the stiffness k with $k^*=k+i\eta k$ in Equation 7.4. (See the note at end of this chapter for the use of complex numbers in solving forced vibration problems.) The force transmitted into the body through a mount with damping is:

$$\left|\frac{F_T}{F}\right| = \frac{\sqrt{1+\eta^2}}{\sqrt{\left(1-\left(\frac{\omega}{\omega_n}\right)^2\right)^2+\eta^2}} = T(\omega) \tag{7.21}$$

where:

F_T = Force transmitted to body through engine mounts

F = Force applied to powertrain

η = Mount structural damping coefficient

As with the undamped powertrain model, isolation begins when $\omega=\omega_n\sqrt{2}$. The peak force transmitted at resonance $\omega=\omega_n$ is reduced as mount damping increases. However, for the isolation region $\omega>\omega_n\sqrt{2}$, as damping increases the force transmitted increases, Figure 7.19. This *control vs. isolation* trade-off requires adjusting damping to balance controlling the amplitude at resonance against the level of vibration isolation achieved.

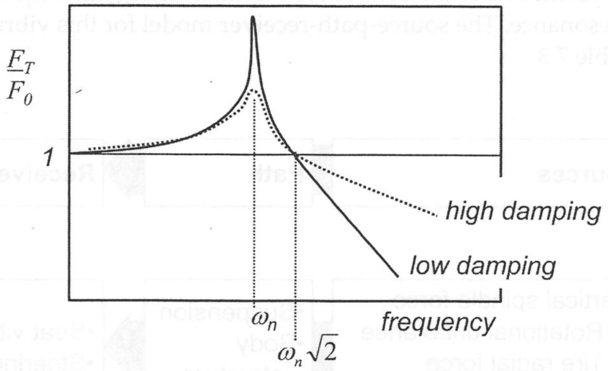

Figure 7.19 Force transmitted into body: Powertrain on rigid base.

The behavior of the powertrain vibratory system is summarized in Figure 7.20. The unbalance force, $F(\omega)$, applied to the powertrain increases as the square of the frequency (slope of +2 on log-log plot). The mounted powertrain acts as an isolator, $T(\omega)$, above ($\omega>\omega_n\sqrt{2}$). Multiplying these two functions yields the force transmitted to the body through the engine mounts, F_T. During design of the body structure, an objective is to position the primary structure resonances—both bending and torsion—in the isolation region.

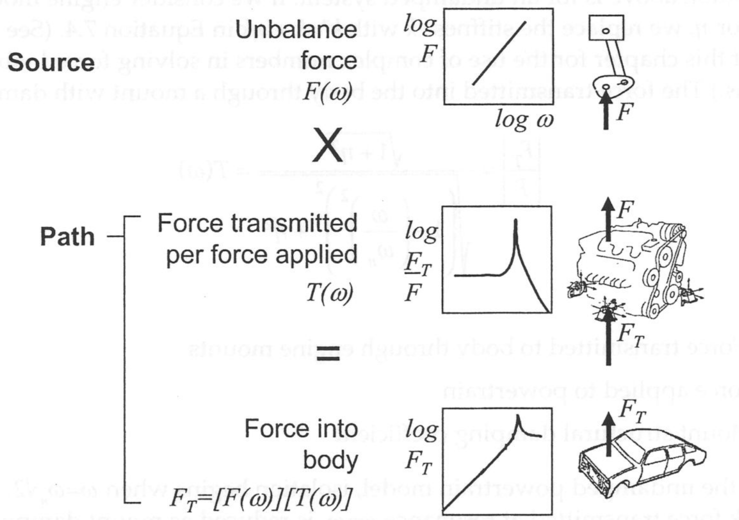

Figure 7.20 Transfer function model of powertrain using log-log plots.

7.4.2 Suspension path: Load at spindle

An important vibration path into the body is through the suspension elements, primarily through the shock absorber and ride spring, Figure 7.21. In general, the suspension system acts as an isolator for vibration energy at frequencies above the wheel hop resonance. The source-path-receiver model for this vibration system is shown in Table 7.3.

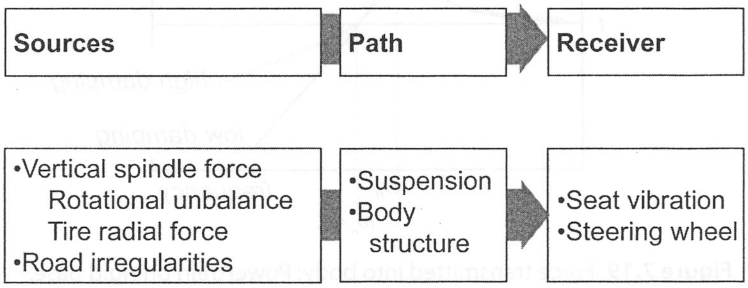

Figure 7.21 Suspension-driven vibration.

Table 7.3 Suspension path vibration system: Load at spindle

Source $F(\omega)$	Isolator $T(\omega)$	Force into Body $F_T(\omega)$	Body Structure Transfer Function $P(\omega)$	Body Deflection $X(\omega)$
Force at suspension spindle	Suspension	Force through shock absorber and ride spring	Body structure	Deflection at seat, steering column

For the purpose of investigating the loads into the body structure, we can model the suspension as a SDOF system, Figure 7.22 [10]. Here the spring is the parallel combination of the ride spring of the suspension and the radial rate of the tire, as measured at the spindle. The mass consists of all elements of the suspension which participate in the vertical motion of the spindle. This mass is primarily the wheel, knuckle, brakes, and the outer portion of the control arms.

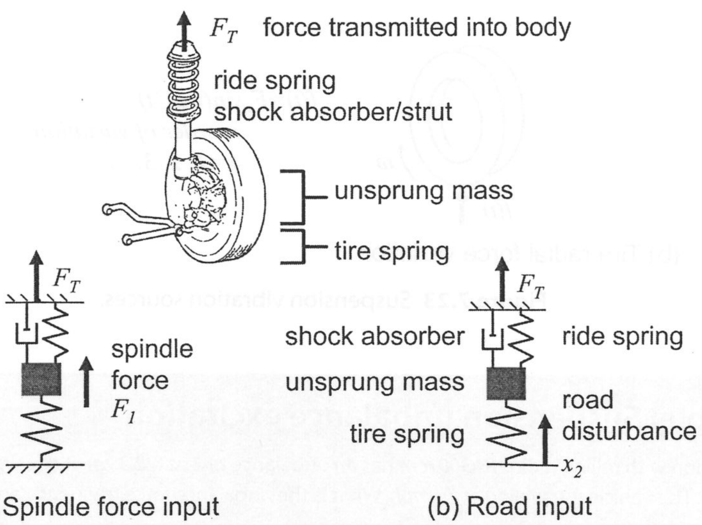

Figure 7.22 First-order model of suspension.

As shown in Figure 7.22a this SDOF may be excited by a load at the spindle. When a wheel unbalance is present, a centrifugal force is applied to the suspension spindle. Generally we are interested in the vertical component of this rotating force, as this is the direction the suspension is most compliant. Figure 7.23a shows this case, with the resulting applied force given by:

$$f(t) = mr\omega^2 \sin \omega t \tag{7.22}$$

where:

$f(t)$ = Vertical force at the spindle

m = Equivalent unbalance mass at wheel rim

r = Wheel rim radius

ω = Rotation speed of wheel [$V=\omega R$, V: vehicle speed, R: tire rolling radius]

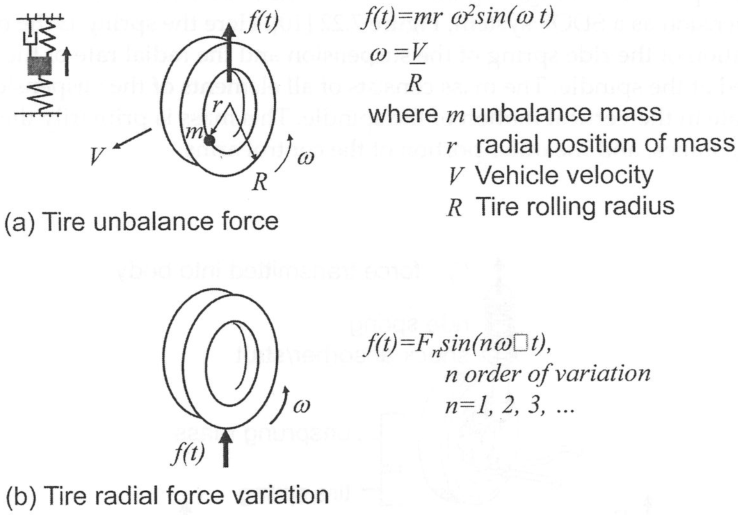

Figure 7.23 Suspension vibration sources.

Example: Suspension unbalance excitation

A suspension with rolling radius *R=300 mm* has an unbalance of *1 oz* (*28.35 g*) at the tire rim of radius *r=170 mm*. The vehicle is traveling at *70 mph*. What is the unbalance force frequency and magnitude?

The frequency is given by:

$$\omega = \frac{V}{R} = \frac{70mi/hr(1.609km/mi)(1000m/km)(1hr/3600\sec)}{300mm(1m/1000mm)} = 104.29 rad/\sec$$

$$f = \frac{\omega}{2\pi} = 16.6 Hz$$

At $\omega=104.29$ *rad/s*, the force amplitude is given by:

$$F = mr\omega^2 = (0.02835kg)(0.170m)(104.29rad/s)^2 = 52.42N$$

A second source for a force applied to the spindle is radial force variation of the tire. Imagine a tire on a test fixture where the spindle is at a fixed distance from an ideally smooth surface, Figure 7.23b. As the tire rolls, the measured vertical force is not constant as expected. Rather we would see some oscillation about the mean force due to imperfections in the tire material and construction. This variation generally has constant amplitude independent of speed, with frequency expressed as multiples (orders) of the rotational speed:

$$f(t) = F_n \sin n\omega t \tag{7.23}$$

where:

n = Vibration order, n=1, 2, 3, . . .

all other variables are the same as Equation 7.22

Under either an unbalance or a radial tire force at the spindle, we may find the resulting spindle deflection for a unit force at the spindle using a free body of the unsprung mass, Figure 7.24 (the use of complex number notation is covered in the note at the end of this chapter):

$$\sum \textit{forces on unsprung mass} = m(\textit{acceleration})$$

$$-X_1k_1 - X_1k_2 - iX_1C\omega + F = m(-X_1\omega^2)$$

$$\frac{X_1}{F} = \frac{1}{k_1 + k_2 - m\omega^2 + iC\omega}$$

$$\frac{X_1}{F} = \frac{\left(\dfrac{1}{k_1+k_2}\right)}{\left(1-\left(\dfrac{\omega}{\omega_n}\right)^2\right)+i\left(\dfrac{C\omega}{k_1+k_2}\right)}$$

$$\left|\frac{X_1}{F}\right| = \frac{\left(\dfrac{1}{k_1+k_2}\right)}{\sqrt{\left(1-\left(\dfrac{\omega}{\omega_n}\right)^2\right)^2+\left(\dfrac{C\omega}{k_1+k_2}\right)^2}} \qquad (7.24)$$

where:

F = Force applied to spindle

k_2 = Ride spring rate

k_1 = Tire spring radial rate

m = Unsprung mass

C = Shock absorber viscous damping factor (typical value is 1000–2000 Ns/m)

ω_n = Wheel hop frequency, $\omega_n = \sqrt{\dfrac{k_1+k_2}{m}}$

$i = \sqrt{-1}$

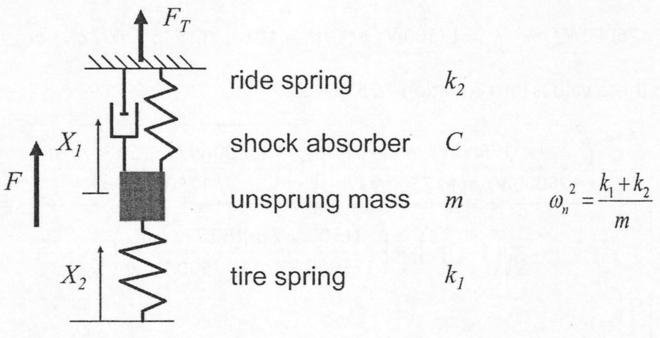

Figure 7.24 First-order suspension analysis.

Example: Wheel hop frequency

For a McPherson strut front suspension as shown in Figure 7.22, a typical tire radial rate is k_1=*175 N/mm*, ride rate k_2=*17.5 N/mm*, and unsprung mass m_1=*40 kg*. The wheel hop frequency for this case is

$$\omega_n = \sqrt{\frac{k_1 + k_2}{m_1}} = \sqrt{\frac{(175+17.5)N/mm(1000mm/m)}{40kg}} = 69.37\,rad/\sec$$

$$f_n = \frac{\omega_n}{2\pi} = \frac{69.37\,rad/\sec}{2\pi} = 11.04Hz$$

This resonance would be excited by a wheel unbalance at a vehicle speed of (rolling radius of *R=300 mm*):

$$V=\omega R=(69.37rad/s)(0.3m)(1km/1000m)(3600s/hr)=74.9kph\ (46.8mph)$$

The suspension acts as an isolator for force transmitted into the body. The force transmitted through the ride spring and shock absorber into the body is $F_T=X_1(k_2+i\omega C)$. Substituting Equation 7.24 into this expression gives:

$$\left|\frac{F_T}{F}\right| = \frac{\left(\frac{k_2}{k_1+k_2}\right)\sqrt{1+\left(\frac{C\omega}{k_2}\right)^2}}{\sqrt{\left(1-\left(\frac{\omega}{\omega_n}\right)^2\right)^2+\left(\frac{C\omega}{k_1+k_2}\right)^2}} = |T(\omega)| \tag{7.25}$$

where:

F_T = Force transmitted to body through shock absorber and ride spring

other variables the same as Equation 7.24

Example: Wheel hop frequency (continued)

For the suspension in the previous example moving at the vehicle speed corresponding to wheel hop ($\omega=\omega_n$), the force transmitted to the body per unit force at the spindle is given by Equation 7.25. For this case the parameters are:

$$k_1 = 175000N/m,\quad k_2 = 17500N/m,\quad m_1 = 40kg,\quad C=1500Ns/m,\quad \omega_n = 69.37r/s$$

Substituting these values into Equation 7.25 gives:

$$\left|\frac{F_T}{F}\right| = \frac{\left(\frac{17500N/m}{175000N/m+17500N/m}\right)\sqrt{1+\left(\frac{(1500Ns/m)(69.37r/s)}{17500N/m}\right)^2}}{\sqrt{\left(1-(1)^2\right)^2+\left(\frac{(1500Ns/m)(69.37r/s)}{175000N/m+17500N/m}\right)^2}} = |T(\omega)|$$

$$\left|\frac{F_T}{F}\right| \cong 1$$

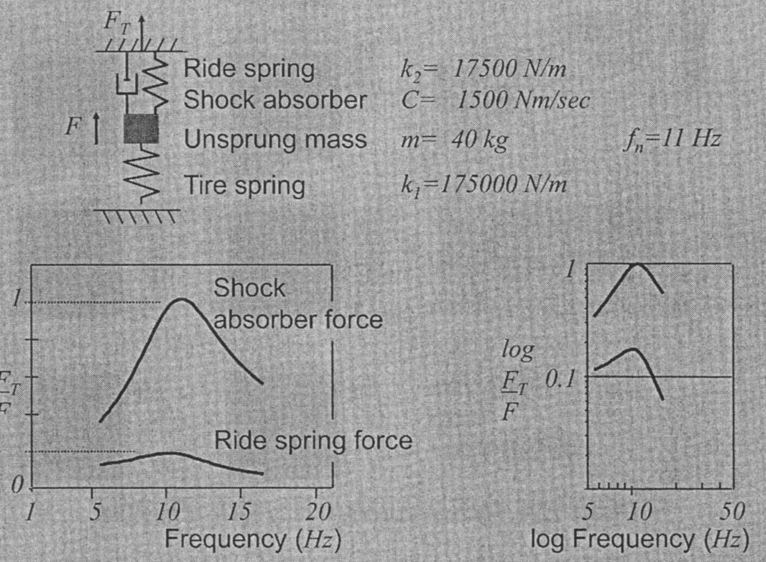

Figure 7.25 Force into body due to unit force at spindle.

This is a peak for the suspension transfer function, and shows that a force applied to the spindle will be passed unattenuated into the body at the wheel hop frequency. Above this frequency, the suspension will attenuate spindle forces (See Figure 7.25 for frequency response in the range *5 Hz<f<15 Hz*. Note that the primary path is though the shock absorber.)

The behavior of this vibratory system is summarized in Figure 7.26. The tire variation spindle force is constant with frequency, while unbalance force increases as the square of the frequency (slope of +2 on the log-log plot). Multiplying these two functions yields the force transmitted to the body through the ride spring/ shock absorber, F_T. Above the wheel hop resonance, the force into the body is less than the force applied to the spindle, and isolation occurs. The primary path for this transmitted force is the shock absorber. During design of the body structure, an objective is to place the primary structure resonances—both bending and torsion— above the wheel hop frequency in the isolation region.

It should be noted that the SDOF suspension model of Figure 7.24 is attached to ground at the ride spring and shock absorber rather than attached to the vehicle rigid-body mass (often called a *quarter car model)*. Therefore the suspension model used here does not exhibit the vehicle ride motions occurring at approximately *1 Hz* and should be applied only for frequencies greater than *5 Hz*. Our model does predict the forces transmitted to the body in the region of wheel hop frequency and above. As these forces are much larger than those occurring at the ride frequencies, our SDOF model is sufficient to understand the isolation behavior of the suspension with respect to the body.

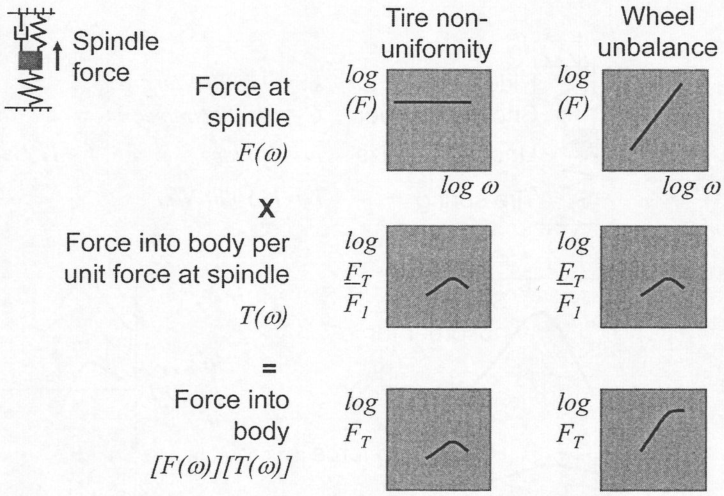

Figure 7.26 Force into body due to force at spindle.

7.4.3 Suspension path: Deflection at tire patch

A second source of vibration flowing through the suspension into the body structure is due to road deflections at the tire patch, Table 7.4.

Table 7.4 Suspension path vibration system: Road input

Source $F(\omega)$	Isolator $T(\omega)$	Force into Body $F_T(\omega)$	Body Structure Transfer Function $P(\omega)$	Body Deflection $X(\omega)$
Road deflection at tire patch	Suspension	Force through shock absorber and ride spring	Body structure	Deflection at seat, steering column

Dynamic characteristics for typical roads have been measured and characterized by the Power Spectral Density (PSD) of the displacement, Equation 7.26 [10]:

$$G = G_0 \frac{\left[1+\left(\frac{\upsilon_0}{\upsilon}\right)^2\right]}{(2\pi\upsilon)^2} \tag{7.26}$$

where:

G = Power Spectral Density $[(m^2)/(cycle/m)]$

υ = Wave number $(cycle/m)$

$G_0 = 1.35 \times 10^{-4}$ Rough Roads, 1.35×10^{-5} Smooth Roads (m^2)

$\upsilon_0 = 0.015$ Bituminous Roads, 0.0061 Concrete Roads $(cycle/m)$

$$f\,(Hz) = \upsilon\,(cycle/m)\; V\,(m/sec) \tag{7.27}$$

where:

υ = Spatial frequency (*cycle/m*)

V = Vehicle speed (*m/sec*)

f = Temporal frequency (*Hz*)

The PSD is a means to characterize a random signal, and may be visualized as the mean-square value of the signal as filtered through a *1 Hz* bandwidth filter at a center frequency *f*. The center frequency is varied over the range of interest to arrive at the full spectrum. For maintained paved roads, Equation 7.26 predicts that the deflection amplitude rapidly diminishes with increasing frequency, Figure 7.27.

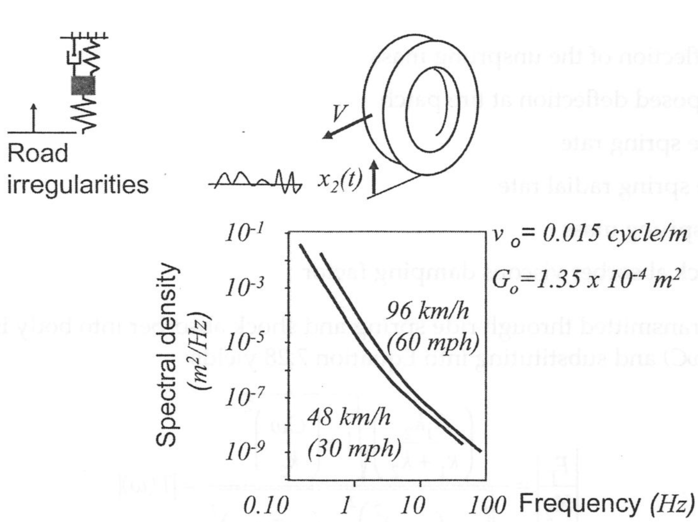

Figure 7.27 Suspension vibration source: Road deflections.

Again, a SDOF model of the suspension may be used to characterize the force transmitted into the body, Figure 7.24. In this model, the input is the displacement at the tire patch, X_2, which may be characterized by the PSD, G, of Equation 7.26. The amplitude of the spindle displacement, X_1, for a unit displacement at the tire patch, X_2, is determined by a free body of the unsprung mass:

$$\sum forces\ on\ unsprung = m(acceleration)$$

$$-(X_1 - X_2)k_1 - X_1k_2 - iX_1C\omega = m(-X_1\omega^2)$$

$$X_2k_1 = (k_1 + k_2 + iC\omega - m\omega^2)X_1$$

$$\frac{X_1}{X_2} = \frac{k_1}{(k_1 + k_2 + iC\omega - m\omega^2)}$$

$$\left|\frac{X_1}{X_2}\right| = \frac{\left(\frac{k_1}{k_1 + k_2}\right)}{\sqrt{\left(1 - \left(\frac{\omega}{\omega_n}\right)^2\right)^2 + \left(\frac{C\omega}{k_1 + k_2}\right)^2}} \quad (7.28)$$

where:

X_1 = Deflection of the unsprung mass

X_2 = Imposed deflection at tire patch

k_2 = Ride spring rate

k_1 = Tire spring radial rate

m = Unsprung mass

C = Shock absorber viscous damping factor

The force transmitted through ride spring and shock absorber into body is $F_T = X_1(k_2 + i\omega C)$ and substituting into Equation 7.28 yields:

$$\left|\frac{F_T}{X_2}\right| = \frac{\left(\frac{k_1k_2}{k_1 + k_2}\right)\sqrt{1 + \left(\frac{C\omega}{k_2}\right)^2}}{\sqrt{\left(1 - \left(\frac{\omega}{\omega_n}\right)^2\right)^2 + \left(\frac{C\omega}{k_1 + k_2}\right)^2}} = |T(\omega)| \quad (7.29)$$

where variables are those of Equation 7.28

The behavior of this vibratory system is summarized in Figure 7.28. Tire patch deflections, $F(\omega)$, rapidly diminish with increasing frequency (slope of –4 on log-log plot). Again the suspension acts as an isolator, $T(\omega)$, and the product of these two functions, $F(\omega)T(\omega)$, yields the force transmitted to the body through the ride spring/shock absorber, F_T. During body structure design, we take advantage of the isolation properties of the suspension by positioning the primary structure resonances—both bending and torsion—above the wheel hop frequency.

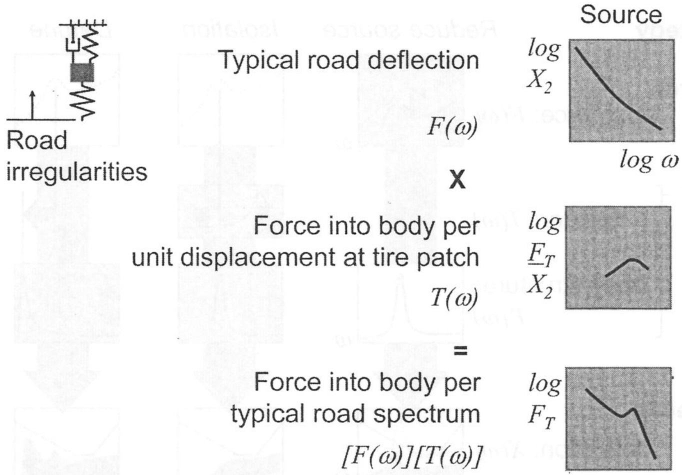

Figure 7.28 Force into body due to road disturbance.

7.5 Strategies for Design for Vibration

We have now characterized some of the major vibration systems for the vehicle. Our design objective is to minimize the source vibration energy flowing to the receiver with undesirable results. Three of the most important strategies to meet this objective are 1) Reduce amplitude of the source; 2) Block the flow of energy using isolators in the path; and 3) Detune resonances in the system [11]. Table 7.5 provides some examples for each of these strategies, and Figure 7.29 illustrates the strategies as log-log frequency response plots.

Table 7.5 Design for vibration strategies.

Strategy	Examples
Reduce amplitude of the vibration source	*Powertrain*
	• Minimize reciprocating mass in engine
	• Add balance shafts to in-line 4 cylinder engine
	Suspension
	• Balance tires
	• High quality tires with low radial force variation
	• Minimize shock absorber forces using a linkage ratio~1
Block the flow of vibration energy using isolators in path	• Mounted powertrain at isolator
	• Suspension as isolator
	• Rubber bushings in chassis links at acoustic frequencies (treated in Section 7.8)
Detune resonances in the system	Positioning body primary bending and torsion resonances to avoid peaks in vibration sources and to take advantage of isolation of mounted powertrain and suspension

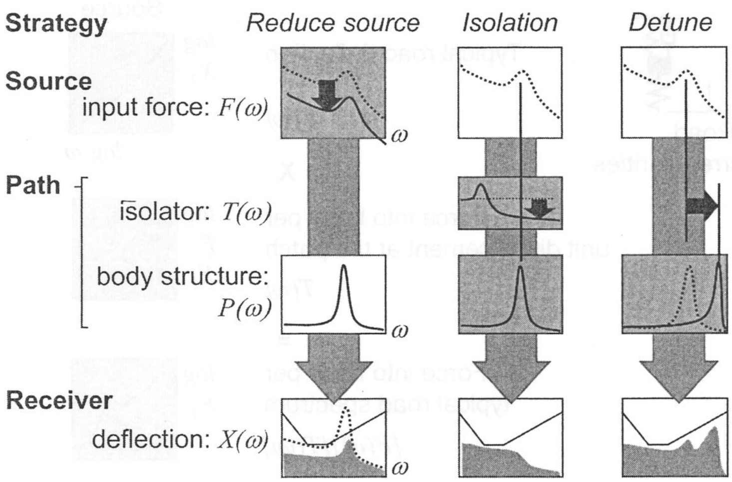

Figure 7.29 Vibration control strategies.

7.5.1 Mode map of vehicle vibratory systems

One of the most important strategies in setting body structure requirements is that of detuning resonances of the body from sources and responders. If this can be achieved during the early design phases, many vibration problems can be avoided, and those remaining may be treated by minor tuning. Using the first-order vibration models of Section 7.4, we can summarize the source, isolator, and responder characteristics for a typical vehicle on a *mode map*, Figure 7.30. This map clearly shows the desirable structural resonance band of *22–25 Hz*. This band falls in the isolation region of the suspension and mounted powertrain, and yet below resonances of downstream paths.

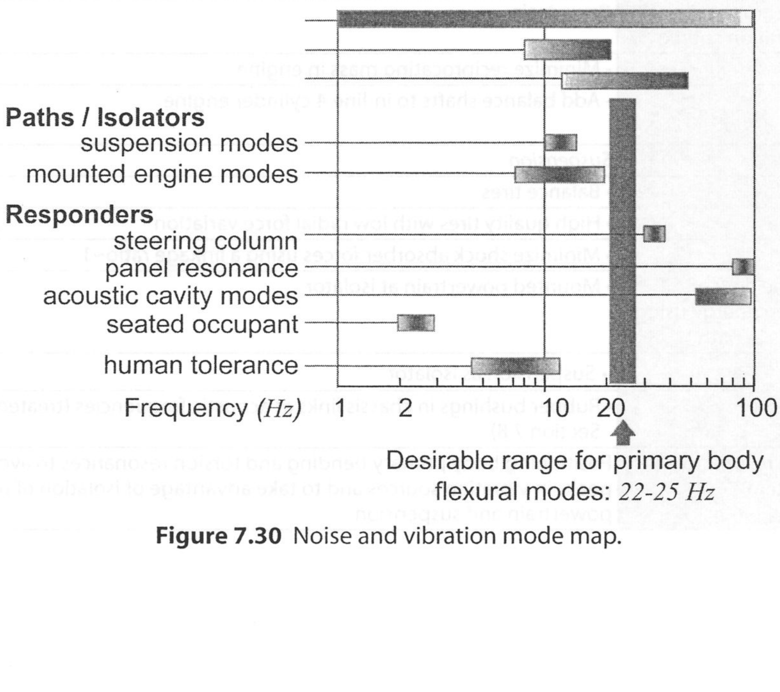

Figure 7.30 Noise and vibration mode map.

7.6 Body Structure Vibration Testing

Often the vibration behavior of an automobile body is evaluated by test. The result of a vibration test is the transfer function, $P(\omega)$, and the deflected shape (mode shape) for each of the resonances. Figure 7.31 shows a typical test set-up [12]. The body shell is suspended on very soft springs such that the rigid body modes occur at low frequencies (<3 *Hz*). This ensures that the rigid modes do not interfere with the flexural resonances to be measured. Often, these support springs are either inflated inner tubes or elastic cords. An electromagnetic or hydraulic shaker is attached to the structure. The forcing location is determined by two criteria: first, the location will excite major modes of vibration (i.e., is not near a nodal point of any important mode). Second, the location is locally stiff (the vibration energy will be directed to the overall mode, not to locally flexing the structure). A typical forcing location is at a front bumper attachment. The shaker is connected to the body through a force transducer and a quill—a very-small-diameter shaft which transmits axial force but does not constrain the body with side loads. An accelerometer is attached to the body at the shaker attachment location to measure the driving point frequency response.

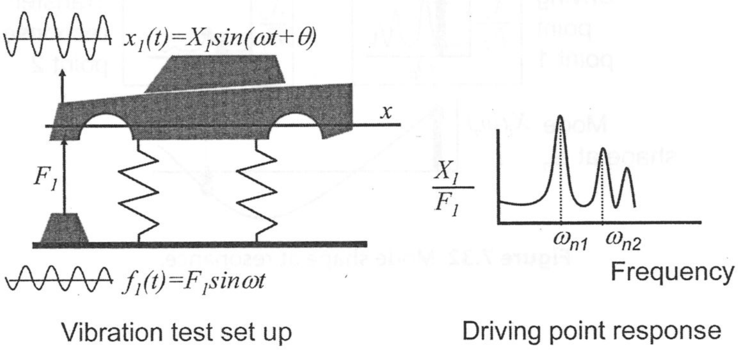

Figure 7.31 Body vibration test.

In practice, a randomly varying force is applied, and the Fourier Transform is taken of the input and output signals resulting in the frequency response. However for visualization purposes, view the input as a sine wave force at a specific frequency. At each frequency, the accelerometer amplitude is plotted while holding the force amplitude fixed. After the frequency has been incremented over a range, the result is a plot of *driving point* response. The peaks on this plot are the resulting body structure resonances.

Now holding the forcing frequency fixed at one of the resonance frequencies, Figure 7.32, the accelerometer location may be moved about the structure and the amplitude recorded for each location. Plotting the amplitude at each location results in a plot of the deflected shape for that resonance—the mode shape, ϕ. The mode shape may be considered a snap-shot taken at the moment when there is maximum deflection throughout the structure. This shape will contain a number of locations with no deflection—nodal points, and a number of locations with greatest deflection—anti-nodes. Note that when a lightly damped structure like the automobile body is excited at a resonance frequency, the motion of all points on the structure are either moving in-phase or 180^o out-of-phase with the driving point.

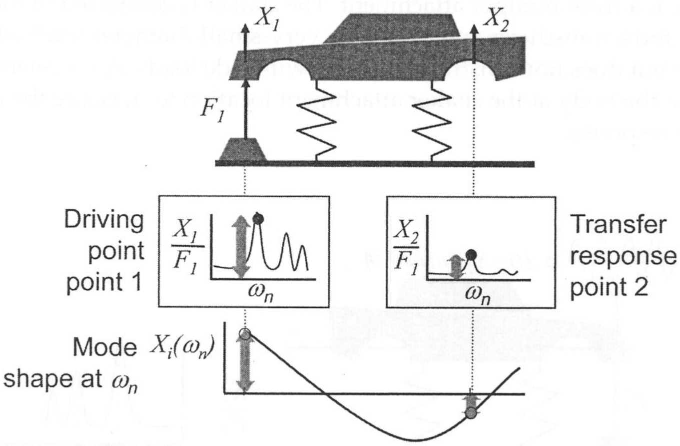

Figure 7.32 Mode shape at resonance.

7.7 Modeling the Body Structure Resonant Behavior

The body structure is a continuous structure with an infinite number of resonant modes, Figure 7.33. The structure's modal density—number of modes occurring in a fixed bandwidth—increases with increasing frequency. For lower frequencies from *10–150 Hz*, individual modes may be characterized using a modal model which we will discuss discussed below. At high frequencies above *1000 Hz*, the modal density is high, with the specific resonant frequencies determined by very small structural details. As these details are subject to manufacturing variability, the precise frequency for the resonance is random. In this high-frequency region, a statistical approach describing the vibration amplitude envelope rather than individual resonances is useful. (The reader is referred to *Machinery Noise and Diagnostics* by R. H. Lyons [13] for more on this approach.) Here we will describe the modal model method for characterizing the lower-frequency flexural modes of the body.

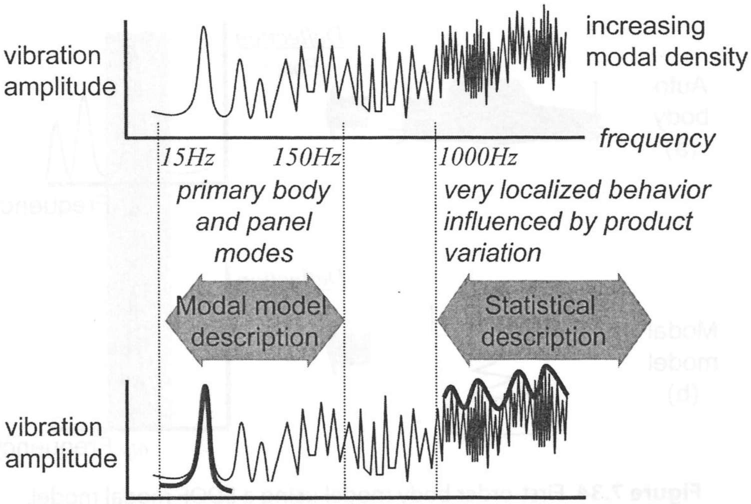

Figure 7.33 Appropriate body model depends on frequency range.

7.7.1 Modal model

The vibration behavior of the primary modes of vibration may be modeled using a *modal model*. In this technique, the behavior around a structural resonance, ω_n, is viewed as a SDOF system.

Consider a body structure of mass, m, with a measured resonant frequency, ω_n, and mode shape ϕ, Figure 7.34a. We can model the behavior of this system with the SDOF system shown in Figure 7.34b. To simulate a load $F_{PHYSICAL}$ applied to the real body structure, we apply a force, F_{MODAL}, to the modal model such that

$$F_{MODAL} = F_{PHYSICAL}\phi_{INPUT} \tag{7.30}$$

where:

$F_{PHYSICAL}$ = Force applied to the physical body structure at the input location

F_{MODAL} = Force applied to the modal model

ϕ_{INPUT} = Influence coefficient at the output (determined from mode shape at resonance at ω_n)

For example, if the physical force is applied near a nodal point *(very small ϕ_{INPUT})*, the modal force will be very small. If the force is applied near an anti-node *(large ϕ_{INPUT})*, then the modal force is large.

In response to this applied modal force, the modal mass oscillates at a deflection amplitude X_{MODAL}. To arrive at the corresponding deflection for the real structure,

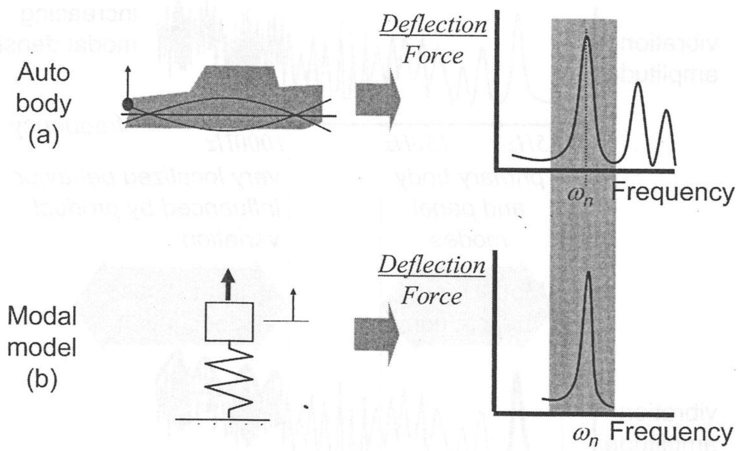

Figure 7.34 First-order body model using a SDOF modal model.

we multiply this modal deflection by the influence coefficient at the output location:

$$X_{PHYSICAL} = X_{MODAL}\phi_{OUTPUT} \tag{7.31}$$

where:

$X_{PHYSICAL}$ = Deflection of the physical body structure at the output location

X_{MODAL} = Deflection of the modal model

ϕ_{OUPUT} = Influence coefficient at the output (determined from mode shape at resonance at ω_n)

Using the relationship for a SDOF transfer function, Equation 7.6, but with the addition of influence coefficients for the input location and output location, the following model results, Figure 7.35:

$$\frac{X_{OUTPUT}}{F_{INPUT}} = \frac{\phi_{OUTPUT}\phi_{INPUT} / k_{MODAL}}{\sqrt{\left(1-\left(\frac{\omega}{\omega_n}\right)^2\right)^2 + (\eta)^2}} \tag{7.32}$$

where:

k_{MODAL} = Modal stiffness: $k—\omega_n^{\ 2}$

ω_n = Model frequency

m_{MODAL} = Modal mass (often set equal to the mass of the body)

η = Modal damping

ϕ_{INPUT} = Input influence coefficient for mode at ω_n

ϕ_{OUTPUT} = Output influence coefficient for mode at ω_n

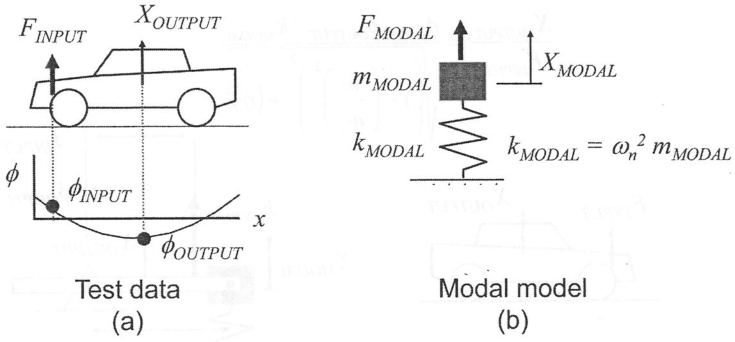

Figure 7.35 Modal model of body.

This modal model represents the behavior in the region of the resonance. We may add the rigid body behavior to extend the model below the resonance region, Figure 7.36. The parameters for this model: ω_n, m_{MODAL}, k_{MODAL}, η, ϕ_{INPUT}, ϕ_{OUTPUT}, may be determined from experimental data.

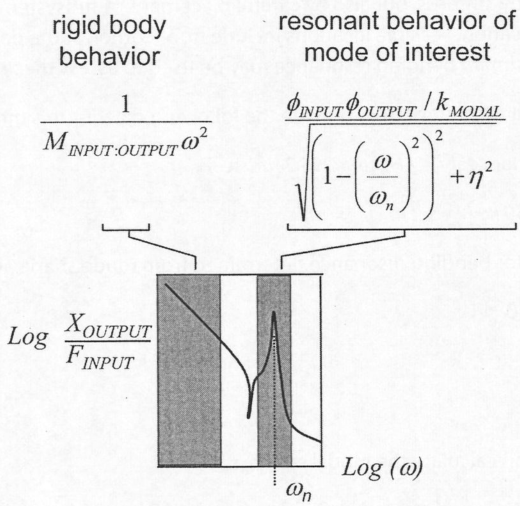

Figure 7.36 Including rigid body behavior in modal model.

A physical interpretation of Equation 7.32 is shown in Figure 7.37 [14]. The modal oscillator is connected to a lever of unit length. The physical force is applied at the lever position ϕ_{INPUT}, and the physical deflection is measured at position ϕ_{OUTPUT}.

$$\frac{X_{OUTPUT}}{F_{INPUT}} = \frac{\phi_{INPUT}\phi_{OUTPUT} / k_{MODAL}}{\sqrt{\left(1-\left(\frac{\omega}{\omega_n}\right)^2\right)^2 + (\eta)^2}}$$

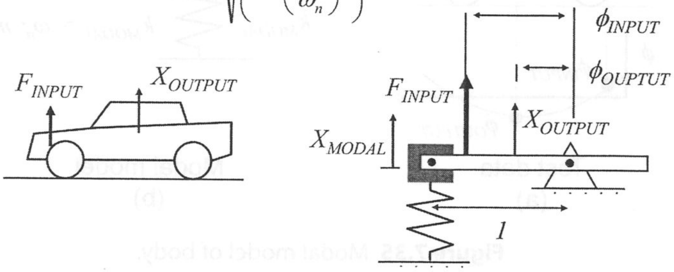

Figure 7.37 Lever analogy for modal model.

Example: Effect of mass placement on structural resonance

A typical design requirement is to place the primary body resonances in the *22–25 Hz* range. Often this involves design changes to increase the resonant frequency from a lower value. We can do this through increased body stiffness, but also by careful placement of subsystem masses. Consider the selection of battery location. Feasible locations include front corner, at the dash, and in the trunk. A modal model of the primary bending resonance may be used to assess these options.

Tests for the body shell without battery provide the following data for this modal model:

Primary bending resonance: $f_n = 47\ Hz$ ($\omega_n = 295.3\ rad/sec$)

Body shell mass: $M = 250\ kg$ (we set $m_{MODAL} = M$)

Influence coefficients for bending resonance determined from mode shape at 47 Hz:

at front corner: $\phi_i = 0.90$

at dash: $\phi_i = -0.20$

at trunk floor: $\phi_i = 0.15$

From these data, we can calculate the modal stiffness:

$$k_{MODAL} = \omega^2 m_{MODAL} = (295.3 rad/\sec)^2 250 kg = 21.8 x 10^6 N/m$$

When we add the battery, the mass of the SDOF modal model is increased, and the new resonant frequency will be

$$f_n = \frac{1}{2\pi}\sqrt{\frac{k_{MODAL}}{m_{MODAL} + m_{EFFECTIVE}}} \quad \text{(A)}$$

where $m_{EFFECTIVE}$ is the effective mass of the battery for this mode of vibration, Figure 7.38. We can determine the effective battery mass by considering the force which a battery of mass, *m*, applies to the car body when at location *i*:

$$F_i = m(\text{acceleration at location } i)$$

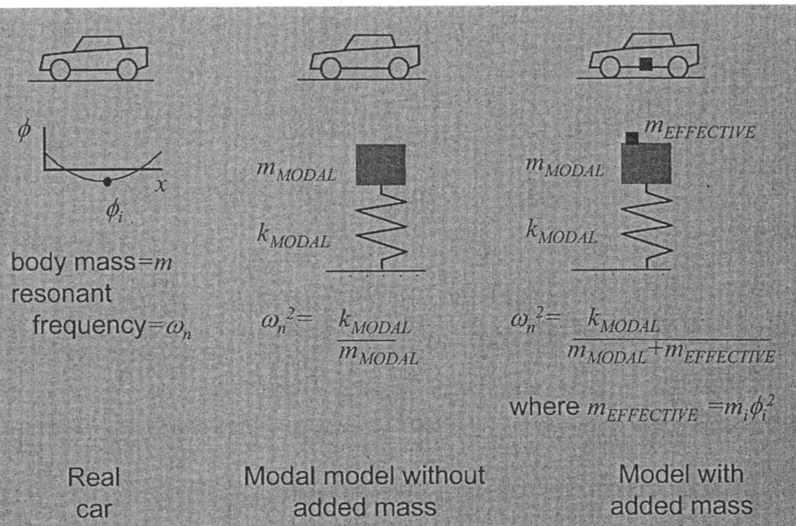

Figure 7.38 Effect on resonant frequency of an added mass.

At the resonant frequency, the acceleration at the battery location is $(X_i\,\omega_n^2)$, where X_i is the deflection amplitude at location i, so

$$F_i—(X_i\,\omega_n^2)$$

Now consider the modal force and acceleration by substituting Equation 7.30 and 7.31 into the above:

$$\frac{F_{MODAL}}{\phi_i} = m(\phi_i X_{MODAL}\,\omega_n^2)$$

$$F_{MODAL} = m\phi_i^2(X_{MODAL}\,\omega_n^2)$$

$$F_{MODAL} = m\phi_i^2(\text{modal acceleration})$$

Inspection of this equation indicates that the effective battery mass for the modal model is

$$m_{EFFECTIVE} = m\phi_i^2$$

Substituting this expression for effective battery mass into Equation A we get an equation for natural frequency of the body structure with the battery mounted:

$$f_n = \frac{1}{2\pi}\sqrt{\frac{k_{MODAL}}{m_{MODAL} + \phi_i^2 m}} \qquad \text{(B)}$$

Substituting the data given, and with a battery mass, $m=16.8\,kg$, we get the following estimates for the primary bending frequency for the battery at each location:

at front corner: $$f_n = \frac{1}{2\pi}\sqrt{\frac{21.8x10^6\,N/m}{250kg+(0.95)^2 16.8kg}} = 45.63\text{Hz}$$

at dash:

$$f_n = \frac{1}{2\pi}\sqrt{\frac{21.8x10^6 N/m}{250kg + (-0.2)^2 16.8kg}} = 46.93\text{Hz}$$

at trunk floor:

$$f_n = \frac{1}{2\pi}\sqrt{\frac{21.8x10^6 N/m}{250kg + (0.15)^2 16.8kg}} = 46.96\text{Hz}$$

This example demonstrates the large influence of component location on primary frequency, Figure 7.39.

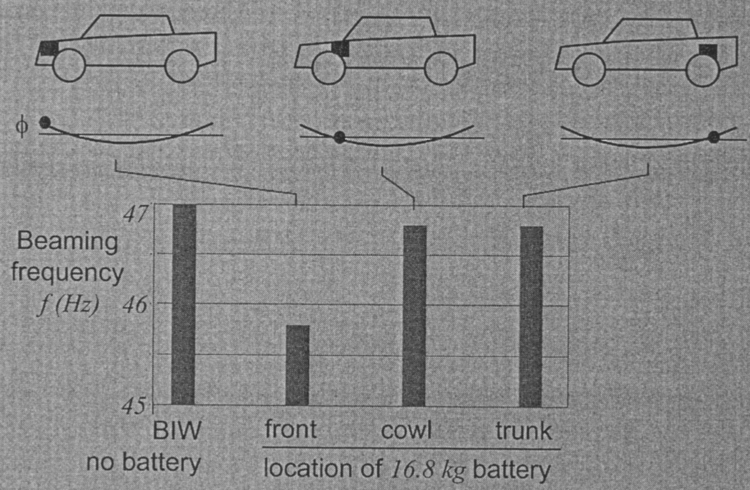

Figure 7.39 Example: Location of battery.

7.8 Vibration at Frequencies Above the Primary Structure Modes

We have been looking at the interaction of vibration sources with the primary body structure resonances in the region *18 Hz to 50 Hz*. At these frequencies, the vibration at the receiver is tactile. At higher frequencies—*50 Hz to 400 Hz*—the response of the body structure is more localized and the vibration is sensed by the receiver acoustically. In this section, we will look at a vibration system in this high-frequency region, Table 7.6, where structure-borne panel vibration excites the air cavity within the vehicle, Figure 7.40.

Table 7.6 Panel vibration system.

Source F(ω)	Body Structure Transfer Function P(ω)	Acoustic Deflection X(ω)
Body panel vibrations	Passenger compartment acoustic resonances	Interior sound pressure

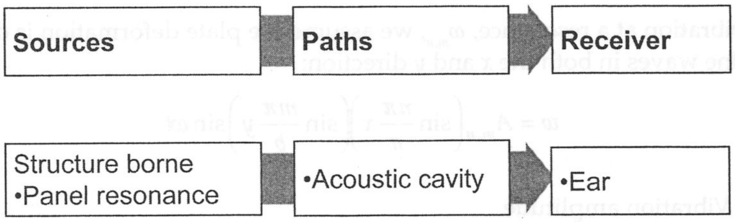

Figure 7.40 Structure- borne vibration.

7.8.1 Body panel vibration

We can model the vibration behavior of a body panel as a flat plate, Figure 7.41. The plate equation below relates the normal deflection of the plate, $w(x, y)$, the plate stiffness, D, and the applied loads, q.

$$\frac{\partial^4 w}{\partial x^4}+2\frac{\partial^4 w}{\partial x^2 \partial y^2}+\frac{\partial^4 w}{\partial y^4}+\frac{q}{D}=0 \tag{7.33}$$

where:

$w(x,y)$ = Normal deflection of the plate

$D=\dfrac{Et^3}{12(1-\mu^2)}$ Plate stiffness

$q(x,y)$ = Normal load per unit of area at location (x, y)

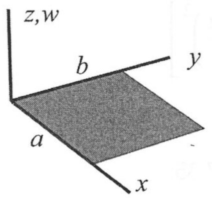

Let deflected shape be:

$w = A_o sin(n\pi x/a) sin(m\pi y/b)\ sin\ \omega_n t$

(note similarity to plate buckling shapes)

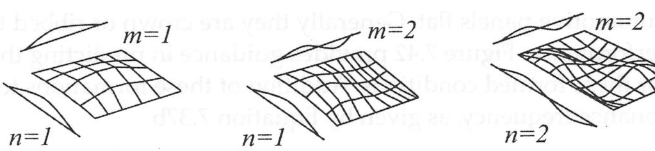

$$\omega_n=\sqrt{\frac{Et^3}{12(1-\mu^2)m''}}\left(\left(\frac{n\pi}{a}\right)^2+\left(\frac{m\pi}{b}\right)^2\right)$$

where
m''=mass per unit area

Figure 7.41 Vibration frequency of a simply supported flat plate.

During vibration at a resonance, $\omega_{m,n}$, we assume the plate deformation is described by half sine waves in both the x and y direction:

$$w = A_{m,n}\left(\sin\frac{n\pi}{a}x\right)\left(\sin\frac{m\pi}{b}y\right)\sin\omega t \qquad (7.34)$$

where:

$A_{m,n}$ = Vibration amplitude

a = Plate length in the x direction

b = Plate width in the y direction

n = Number of half sine waves in the x direction, $n=1, 2,\ldots$

m = Number of half sine waves in the y direction, $m=1, 2,\ldots.$

ω = Vibration frequency (rad/s)

This assumed deformation is appropriate for simply supported boundary conditions. The normal load, q, is that of the inertia force of a small patch of plate:

$$q = m''\frac{\partial^2 w}{\partial t^2} \qquad (7.35)$$

where m'' = Plate mass per unit area

Substituting the deflected shape, Equation 7.34, and 7.35 into Equation 7.33 yields:

$$\left[\left(\frac{n\pi}{a}\right)^4 + 2\left(\frac{n\pi}{a}\right)^2\left(\frac{m\pi}{b}\right)^2 + \left(\frac{m\pi}{b}\right)^4 - \frac{\omega^2 m''}{D}\right]\left[A_{m,n}\left(\sin\frac{n\pi}{a}x\right)\left(\sin\frac{m\pi}{a}y\right)\sin\omega\right] = 0 \qquad (7.36)$$

To satisfy this equality, the first bracketed term must be zero at the resonant frequencies. Solving for the frequency yields

$$\omega_{m,n} = \pi^2\sqrt{\frac{D}{m''}}\left[\left(\frac{n}{a}\right)^2 + \left(\frac{m}{b}\right)^2\right] \qquad (7.37a)$$

where:

$\omega_{m,n}$ = Resonant frequency

other variables defined in Equations 7.33, 7.34, & 7.35

Rarely are automotive panels flat. Generally they are crown or ribbed to enhance structural performance. Figure 7.42 provides guidance in predicting the resonant frequency for these formed conditions. Addition of these formations to a panel will increase resonance frequency, as given by Equation 7.37b

$$\frac{f_{FORMED}}{f_{FLAT}} = C\sqrt{\frac{H_C}{t}} \qquad (7.37b)$$

where:

f_{FORMED} = Formed panel primary frequency

f_{FLAT} = Flat panel primary frequency given by Equation 7.37a with $m=n=1$

H_C = Crown height

t = Panel thickness

C = Constant ($C=1.25$ for crown, $C=1$ for ribbed panel)

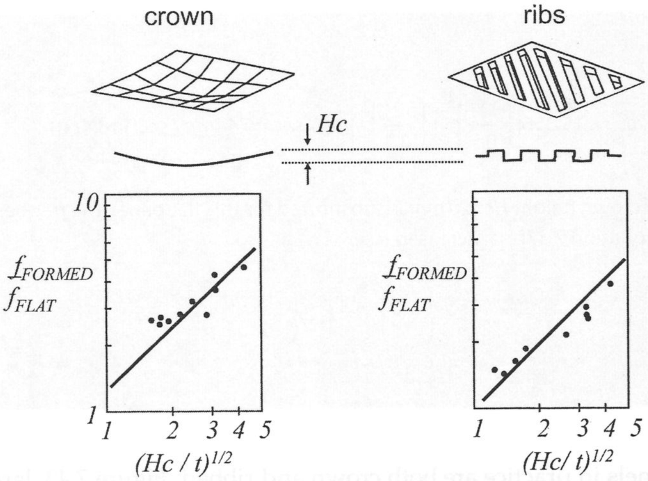

Figure 7.42 Experimental plate stiffening study.

Example: Vibration frequencies for floor pan

The floor pan at the rear foot well may be considered a flat panel of dimensions *a=500 mm* and *b=300 mm*. For a steel panel with thickness *t=1 mm*, the plate stiffness is:

$$D = \frac{Et^3}{12(1-\mu^2)} = \frac{(207000N/mm^2)(1mm)^3}{12(1-0.3^2)}$$
$$= 18956Nmm(1m/1000mm) = 18.956Nm$$

and the mass area density is:

$$m'' = \rho t = (7.83 \times 10^{-6} kg/mm^3)(1mm)$$
$$m'' = (7.83 \times 10^{-6} kg/mm^2)(1000mm/m)^2 = 7.83kg/m^2$$

Using Equation 7.37 yields:

$$\omega_{m,n} = \pi^2 \sqrt{\frac{D}{m''}} \left[\left(\frac{n}{a}\right)^2 + \left(\frac{m}{b}\right)^2 \right] = \pi^2 \sqrt{\frac{18.956Nm}{7.83kg/m^2}} \left[\left(\frac{n}{0.5m}\right)^2 + \left(\frac{m}{0.3m}\right)^2 \right]$$

$$\omega_{m,n} = 15.356 \left[\left(\frac{n}{0.5}\right)^2 + \left(\frac{m}{0.3}\right)^2 \right] rad/\sec$$

for *m=1, n=1*:

$$\omega_{1,1} = 15.356 \left[\left(\frac{1}{0.5}\right)^2 + \left(\frac{1}{0.3}\right)^2 \right] rad/\sec = 232 rad/\sec (36.9Hz)$$

for $m=2, n=1$:

$$\omega_{12} = 15.356\left[\left(\frac{1}{0.5}\right)^2 + \left(\frac{2}{0.3}\right)^2\right] rad/\sec = 744 rad/\sec(118.4 Hz)$$

If a crown panel of crown height $Hc=20\ mm$ is substituted for this flat panel, the frequency of the first mode, using Equation 7.37b, is increased to

$$\frac{f_{FORMED}}{f_{FLAT}} = 1.25\left(\frac{H_c}{t}\right)^{1/2} = 1.25\left(\frac{20mm}{1mm}\right)^{1/2} = 5.59$$

$$f_{FORMED} = 5.59(36.9 Hz) = 206 Hz$$

Automotive panels in practice are both crown and ribbed, Figure 7.43, largely due to this ability to increase panel resonant frequencies [15].

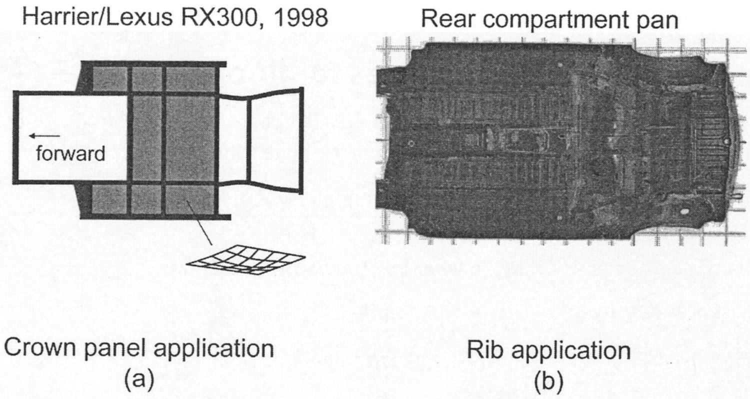

Figure 7.43 Panel stiffening to increase vibration frequency. (Photo courtesey of A2Mac1.com, Automotive Benchmarking)

7.8.2 Acoustic cavity resonance

The closed air cavity of the passenger compartment can resonate with a standing acoustic wave similar to an organ pipe, Figure 7.44. In this case, the boundary conditions at either end are closed. For this condition the acoustic resonant frequency is given by:

$$f_n \lambda = c \qquad (7.38)$$

where:

f_n = Resonant frequency (Hz)

λ = Wavelength

c = Speed of sound in air (~$330\ m/sec$)

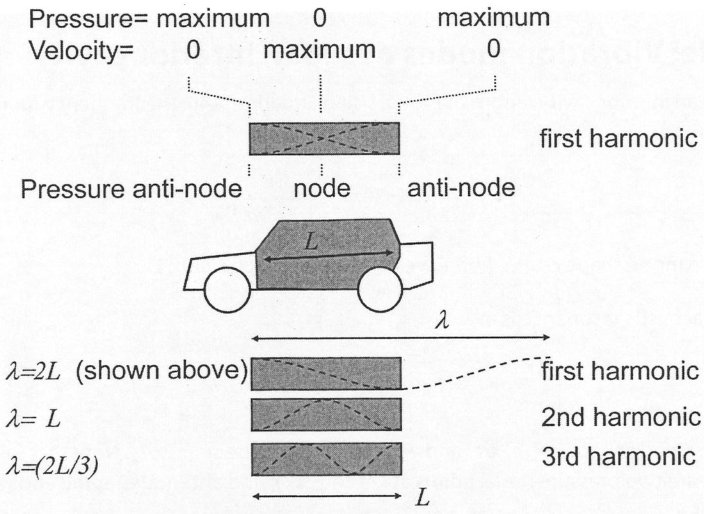

Figure 7.44 Cavity resonance.

The standing wavelength is

$$\lambda = \frac{2L}{n} \tag{7.39}$$

where:

L = Cabin length

n = Number of half cosine waves along cabin length, $n=1, 2, 3 \ldots$

Substituting Equation 7.39 into 7.38 yields:

$$f_n = c\left(\frac{n}{2L}\right) \tag{7.40}$$

At each resonance the *pressure* mode shape is given by the cosine function, $cos(\pi nx/L)$, where x is the length coordinate with origin at the front of the cavity. For example, at the first acoustic resonance, $n=1$, the pressure amplitude is maximum (anti-node) at either end of the passenger compartment and zero (node) at the midpoint. The pressure mode shape gives some notion of the sound level. For this case, with a midpoint node the sound pressure level at the driver's ear is low.

The air *velocity* mode shape is given by $sin(\pi nx/L)$. The velocity mode shape provides an indication of the sensitivity of the cavity mode to excitation by a panel. A panel located near the velocity anti-node will excite the cavity resonance to a high degree.

Example: Vibration modes of sedan interior cavity

A sedan has an interior cavity length of *L=3 m*. Using Equation 7.40, the frequency for first acoustic resonance is:

$$f_n = c\left(\frac{n}{2L}\right) = (330m/s)\left(\frac{1}{2\cdot 3m}\right) = 55Hz$$

with pressure mode shape *cos(πx/L)*, and velocity mode shape *sin(πx/L)*.

The second acoustic resonance is at

$$f_n = 330m/s\left(\frac{2}{2\cdot 3m}\right) = 110Hz$$

with pressure mode shape *cos(π2x/L)* and velocity mode shape *sin(π2x/L)*. Note that for this second mode, there are two pressure nodal points at *L/4* and *3L/4*, and anti-nodes at the ends as well as at the midpoint.

The two examples above illustrate the source-path-receiver system in which panel vibration becomes a vibration source, exciting cavity resonances, causing sound pressure at the driver's ear, Figure 7.45. For these examples, the flat panel resonance at *118.4 Hz* will couple with the air cavity resonance at *110 Hz* resulting in high sound pressure levels at the driver's ear. By crowning the panel, the panel resonant frequency will increase and would become detuned from the acoustic resonance resulting in a reduced sound level.

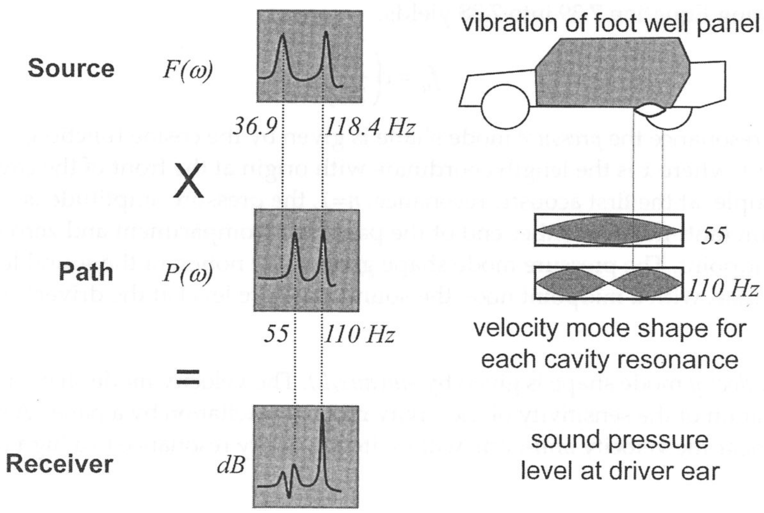

Figure 7.45 Panel and acoustic cavity as vibration system.

Table 7.7 Suspension element noise path vibration system.

Source $F(\omega)$	$T(\omega)$	$F_T(\omega)$	$P(\omega)$	$X(\omega)$
High-frequency chassis deflections	Chassis links with end bushings	Body panel vibrations	Passenger compartment acoustic resonances	Interior sound pressure

7.8.3 Vibration isolation through elastomeric elements

We can now expand the vibration system of the previous section by including a typical isolator in the path, Table 7.7 and Figure 7.46. High frequency deflections may occur in suspension elements due to road impacts. To isolate these higher-frequency vibrations, the suspension elements have elastomeric bushings at the body connections, Figure 7.47.

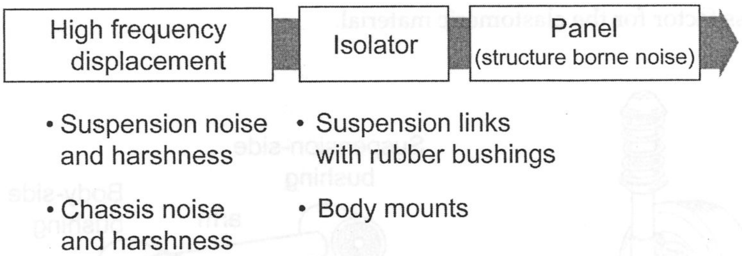

Figure 7.46 Role of isolators in higher-frequency vibration.

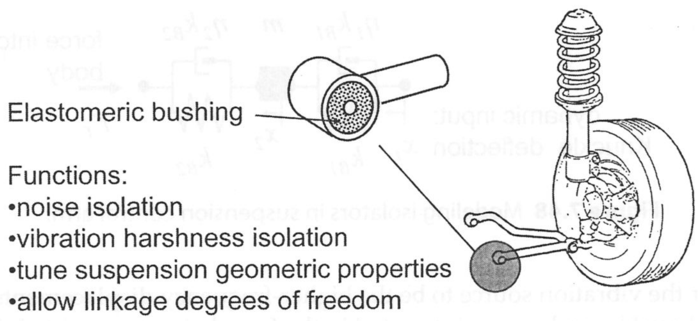

Figure 7.47 Lower control arm bushing.

To understand how these bushings help reduce vibration into the body, consider the model shown in Figure 7.48 [16]. A suspension lower control arm is shown. At either end of the arm, the connection is through an elastomeric bushing. The bushings may be viewed as a stiffness element and damping element in parallel. This may be modeled as a complex stiffness, k^*, with the imaginary part indicating the bushing damping. *(See note at end of this chapter on using rotating phasors to model vibration systems.)* The bushing behavior can then be written as:

$$\begin{aligned} F &= kX + i\eta kX = k^* X \\ \frac{F}{X} &= (k + i\eta k) = k^* \\ \frac{F}{X} &= (\mathit{Stiffness\ Portion}) + i(\mathit{Damping\ Portion}) \end{aligned} \tag{7.41}$$

where:

F = Force through the bushing

X = Deflection across the bushing

η = Loss factor for the elastomeric material.

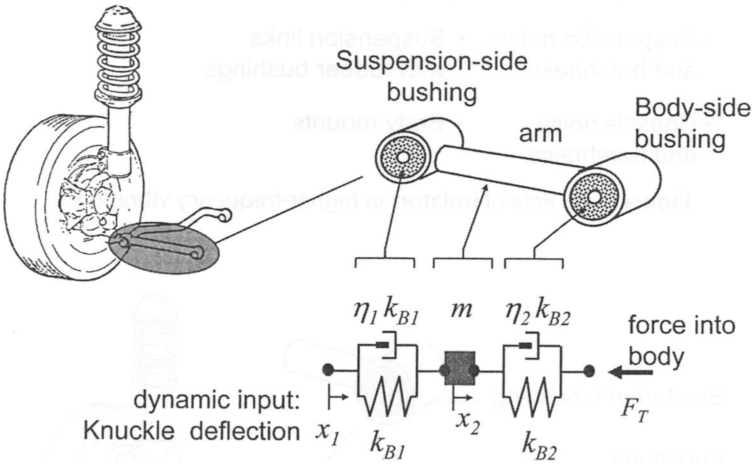

Figure 7.48 Modeling isolators in suspension control arm.

We consider the vibration source to be the higher-frequency displacements of the suspension knuckle, and we are interested in the force being transmitted through the body-side bushing into the body structure. This transfer function, $T(\omega)=F_T/X$, is given by:

$$\frac{F_T}{X} = \frac{\left(\dfrac{k^*_{B1} k^*_{B2}}{k^*_{B1} + k^*_{B2}}\right)}{1 - \omega^2 \dfrac{m}{\left(k^*_{B1} + k^*_{B2}\right)}} \tag{7.42}$$

where:

k^*_{B1} = Suspension-side bushing stiffness $k^*_{b1}=(k_{B1}+i\eta_1 k_{B1})$

k^*_{B2} = Body-side bushing stiffness $k^*_{B2}=(k_{B2}+i\eta_2 k_{B2})$

m = Mass of the chassis link

F_T = Vibration force amplitude transmitted into body structure

X = Vibration displacement amplitude imposed by suspension knuckle

At very low frequencies ($\omega \approx 0$), Equation 7.42 tells us that the combined link stiffness is the series combination of the two bushing stiffnesses:

$$\left.\frac{F_T}{X}\right|_{\omega \approx 0} = \left(\frac{k_{B1}k_{B2}}{k_{B1}+k_{B2}}\right) \tag{7.43}$$

At a frequency of

$$\omega_n = \sqrt{\frac{(k_{B1}+k_{B2})}{m}} \tag{7.44}$$

the chassis link resonates against the two bushings. We can expand Equation 7.42 by substituting in the complex stiffness expressions of Equation 7.41 and arrive at

$$\left|\frac{F_T}{X_1}\right| = \left(\frac{k_{B1}k_{B2}}{k_{B1}+k_{B2}}\right)\left(\frac{\sqrt{1+\eta^4}}{\sqrt{\left(1-\left(\frac{\omega}{\omega_n}\right)^2\right)^2+\eta^2}}\right) = |T(\omega)| \tag{7.45}$$

where:

η = Loss factor at each bushing

other variables are those of Equation 7.42

The first bracketed expression in Equation 7.45 is the static stiffness. The second expression is the gain at frequency ω. For the damping levels usually seen in bushings ($\eta<0.2$), the η terms in Equation 7.45 vanish. We then see that for frequencies above $\sqrt{\omega_n}$ the force transmitted through the link begins to be attenuated over that transmitted statically (*gain*<1). The chassis link acts as an isolator for the higher-frequency vibrations, Figure 7.49. Notice also in this figure that there is a trade-off due to bushing damping; high damping controls the amplitude at resonance, but increases the force transmitted at higher frequencies.

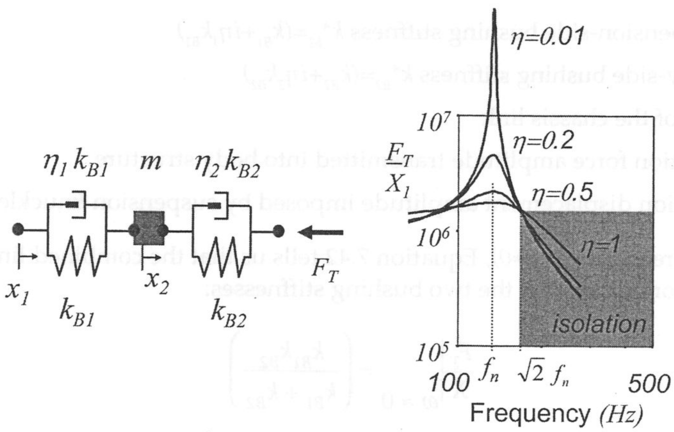

Figure 7.49 Response of isolators in suspension control arm.

Example: Suspension lower control arm

A source of high-frequency vibration is due to gear meshing in the transmission. This vibration is transmitted through the front wheel drive shaft to the suspension knuckle. The knuckle vibration is then transmitted though the suspension control arm (chassis link) into the body structure.

For this example consider a mesh frequency of *400 Hz*. To see how the lower control arm with bushings can attenuate this vibration, consider the following values: Identical bushings at either end of the control arm with stiffness $k_{B1}=k_{B2}=175000\ N/m$ and loss factor $\eta=0.2$, control arm mass of $m=5\ kg$, and excitation frequency $f=400\ Hz$.

For very low frequencies ($f\approx 0\ Hz$), the force transmitted to the body per unit of knuckle deflection is given by:

$$\frac{F_T}{X}=\left(\frac{k_{B1}k_{B2}}{k_{B1}+k_{B2}}\right)$$

$$\frac{F_T}{X}=\left(\frac{(1750000N/m)(1750000N/m)}{1750000N/m+1750000N/m}\right)=875000N/m$$

The natural frequency of this bushing/arm SDOF is

$$\omega_n=\sqrt{\frac{(k_{B1}+k_{B2})}{m}}$$

$$\omega_n=\sqrt{\frac{(1750000N/m+1750000N/m)}{5kg}}=836.7r/s\quad(133Hz)$$

Now consider the force transmitted per unit of knuckle deflection at *f=400 Hz* given by:

$$\left|\frac{F_T}{X_1}\right| = \frac{\left(\dfrac{k_{B1}k_{B2}}{k_{B1}+k_{B2}}\right)\sqrt{1+\eta^4}}{\sqrt{\left(1-\left(\dfrac{\omega}{\omega_n}\right)^2\right)^2+\eta^2}}$$

$$\left|\frac{F_T}{X_1}\right| = \frac{\left(\dfrac{k_{B1}k_{B2}}{k_{B1}+k_{B2}}\right)\sqrt{1+0.2^4}}{\sqrt{\left(1-\left(\dfrac{400\,Hz}{133\,Hz}\right)^2\right)^2+0.2^2}} = 0.125\left(\frac{k_{b1}k_{b2}}{k_{b1}+k_{b2}}\right)$$

The arm attenuates the dynamic force into the body by a factor of *0.125* at *400 Hz*.

Example: High-frequency powertrain vibration through engine mount

On some vehicles, the powertrain is mounted directly to the body structure through engine mounts (rather than to a softly mounted cradle). In this direct-mounted case, high-frequency vibration of the engine block may be transmitted through the engine mount to the body, resulting in structure-borne noise. In this example, it was desired to increase the engine spark timing for improved fuel economy. This change in timing increased the dynamic block deflections in the *400–2000 Hz* range, Figure 7.50. To isolate these acoustic vibrations from the body, an engine mount consisting of a free mass was used, Figure 7.51b [17] (a conventional mount is shown for comparison in Figure 7.51a). The model for this mount, also shown in Figure 7.51b, is identical to that of the suspension link discussed above. The desired static stiffness was *200 N/mm*. From Equation 7.43 the stiffness for the two identical bushings can be found:

$$\frac{F_T}{X} = \left(\frac{k_{B1}k_{B2}}{k_{B1}+k_{B2}}\right) = 200\,N/mm$$

$$k_{B1} = k_{B2} = 400\,N/mm$$

It was desired to begin isolation at *270 Hz*. Therefore

$$270\,Hz = \sqrt{2}f_n$$

$$f_n = 190\,Hz$$

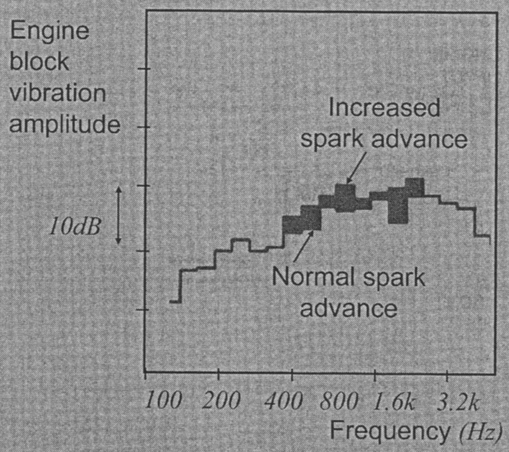

Figure 7.50 Acoustic deflections of powertrain.

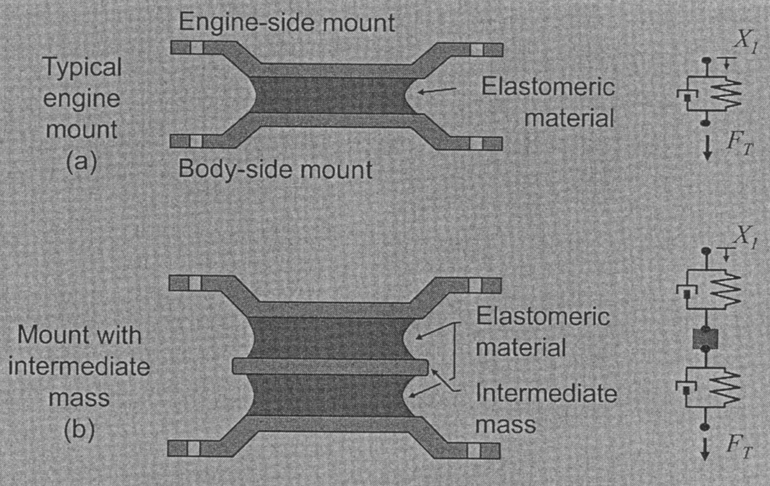

Figure 7.51 Engine mount concepts.

Equation 7.44 can be rearranged to calculate the needed intermediate mass:

$$\omega_n = \sqrt{\frac{\left(k_{B1}+k_{B2}\right)}{m}}$$

$$m = \frac{2k_B}{\omega_n^2} = \frac{2(400000N/m)}{(2\pi 190 rad/\sec)^2} = 0.56kg$$

This mount will support the powertrain at the required static rate and additionally act as a filter for the higher-frequency vibration, Figure 7.52.

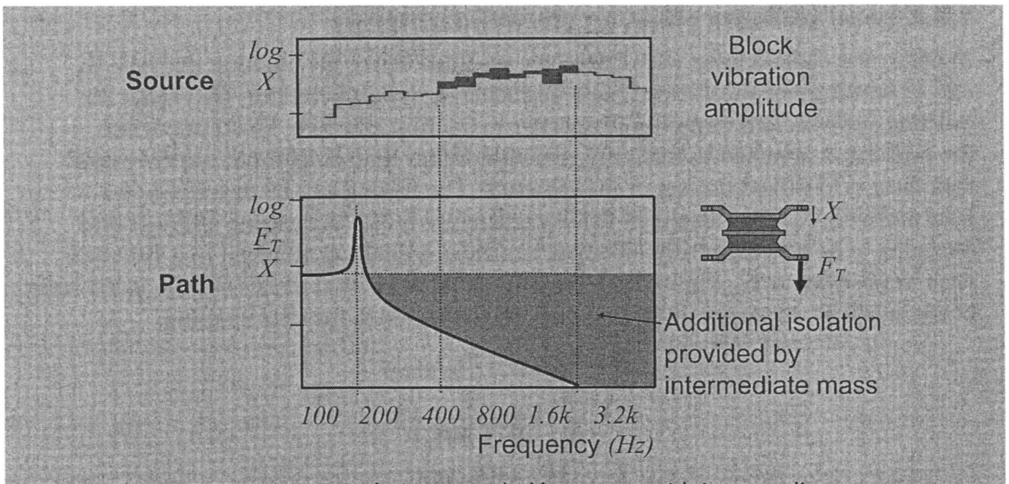

Figure 7.52 Acoustic isolation provided by mount with intermediate mass.

Many additional connections within the vehicle may be viewed as elastomeric elements with an intermediate mass. For example, Figure 7.53 shows a body-frame interface connected through an elastomeric body mount.

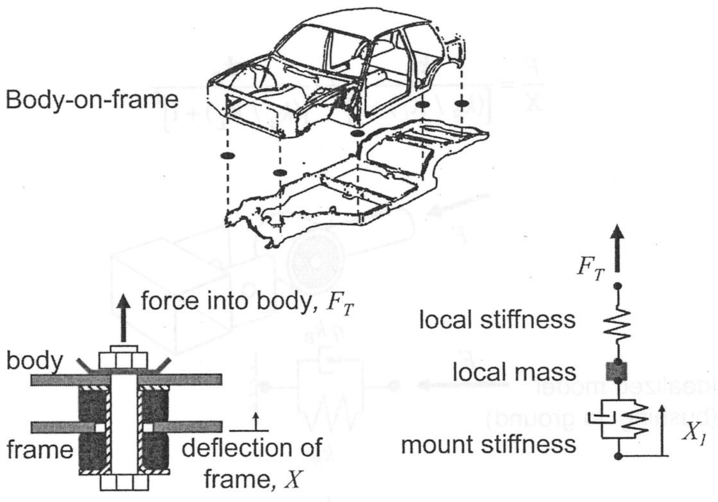

Figure 7.53 Body mount isolation behavior.

7.8.4 Local stiffness effect on vibration isolators

In designing chassis links with bushings, we must select the bushing material (k_b and η) which gives the desired high-frequency-isolation behavior. We expect the bushing stiffness and damping properties to be fully effective. However, when the bushing is attached to the body structure rather than to ground, we have seen that there is localized flexing of the structure. The flexing can be described as a local stiffness, K_L. This localized flexing will cause both the bushing stiffness and damping to be less than fully effective. Consider a bushing attached to a structure with local stiffness, K_L, Figure 7.54. Now the total deflection of this system is the sum of the localized structure deflection and the deflection across the bushing:

$$X = X_{LOCAL} + X_{BUSHING}$$

$$X = \frac{F}{K_L} + \frac{F}{k_B + i(\eta k_B)}$$

$$\frac{F}{X} = \frac{kK_L + i(K_L k\eta)}{(k_B + i\eta k_B + K_L)}$$

Which can be rearranged to

$$\frac{F}{X} = \frac{k_B\left[(k_B / K_L) + 1 + \eta^2 (k_B / K_L)\right] + i(\eta k_B)}{\left[(k_B / K_L) + 1\right]^2 + \left[\eta (k_B / K_L)\right]^2} \qquad (7.46)$$

The loss factor, η, is typically $0<\eta<0.2$ and we can make the approximation $\eta^2 \sim 0$ giving:

$$\frac{F}{X} = \frac{k_B}{\left[(k_B / K_L) + 1\right]} + i\frac{\eta k_B}{\left[(k_B / K_L) + 1\right]^2} \qquad (7.47)$$

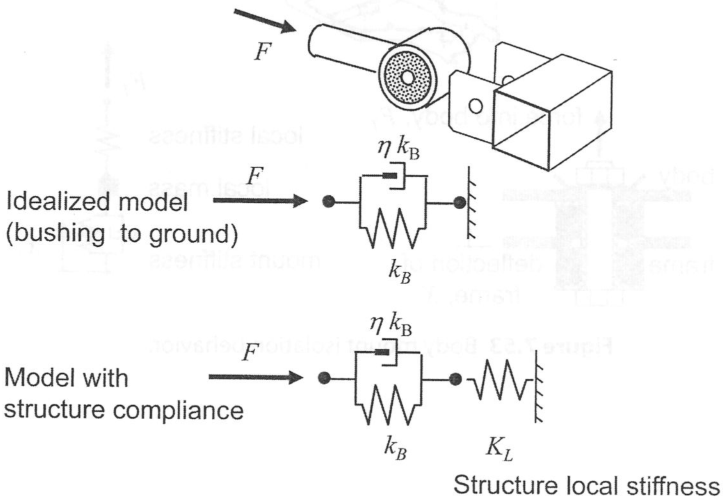

Figure 7.54 Isolator attachment to flexible structure.

Compare this final expression to the expression for a bushing attached to ground:

$$\frac{F}{X} = k_B + i\eta k_B$$

We can see that the stiffness portion of Equation 7.47—the real component—is reduced by a factor of:

$$\frac{1}{[(k_B / K_L) + 1]}$$

However the damping portion of Equation 7.47—the imaginary component—is reduced by a factor of:

$$\frac{1}{[(k_B / K_L) + 1]^2}$$

Thus, when the body structure has local flexibility at a bushing attachment, the damping qualities of the bushing are reduced more than that of the stiffness, Figure 7.55. This result has implications for structure design at attachments where we expect high-frequency inputs; the local stiffness of the structure, K_L, should be at least five times the bushing stiffness, k_b, to maintain *70%* of the bushing damping.

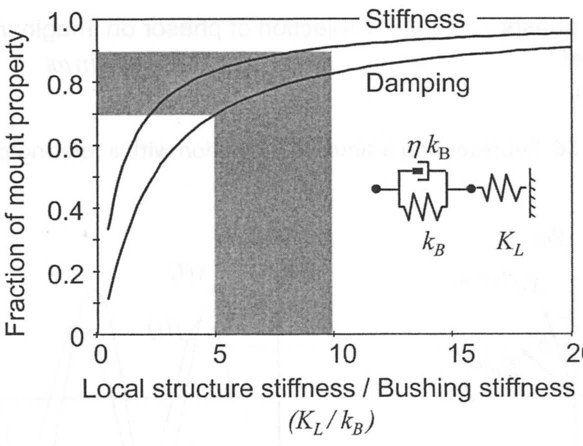

Figure 7.55 Required local stiffness for effective isolation.

7.8.5 Summary: Design for vibration

In this chapter, we have looked at a few of the important vibratory systems in the automobile. Our focus has been on determining the required qualities of the body structure which will minimize objectionable vibration levels. During early design layout, it is important to detune structural resonances from source vibrations, and also to take advantage of the isolation characteristics of other systems, suspension and mounted powertrain, for example. For preliminary design, this detuning can be achieved using the first-order models presented in this chapter.

7.9 Note on Use of Rotating Phasors to Solve Damped Vibration Problems

Earlier in this chapter we used complex variables to describe damping behavior. In this section we will further develop this useful concept. Consider a vector of length X rotating about a fixed point at a rotation speed of ω *rad/sec*, Figure 7.56a [18]. The projection of this vector onto the vertical axis can be described by $x(t)=X\sin\omega t$, Figure 7.56b. Now consider the horizontal axis to be the *Real axis* and the vertical axis to be the *Imaginary axis*. The vector may be described as the rotating phasor $x(t)=Xe^{i\omega t}$. If we also let the amplitude of the phasor X be complex $X^{*}=(X_{Re})+i\,(X_{Im})$, then the phase angle, θ is given by $\tan^{-1}(X_{Im}m/X_{Re})$, Figure 7.57. This visualization offers some simplifications in solving damped vibration problems.

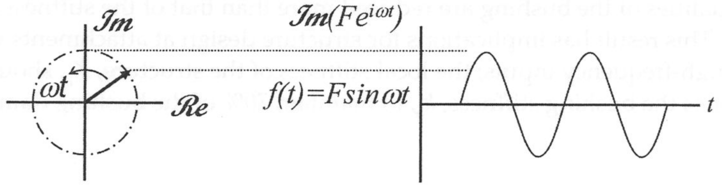

Rotating phasor $Fe^{i\omega t}$ (a)

Projection of phasor on imaginary axis $\mathcal{I}m(Fe^{i\omega t})=F\sin\omega t$ (b)

Figure 7.56 Representing a sinusoidal function with a rotating phasor.

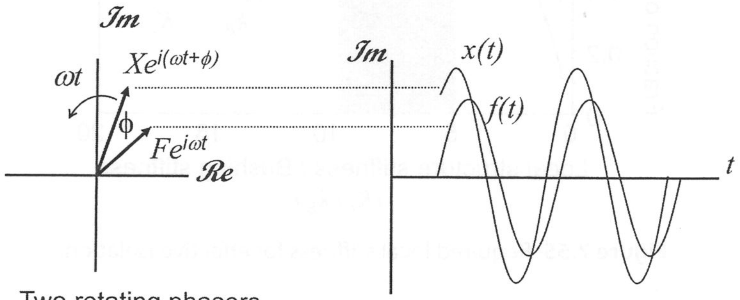

Two rotating phasors ($Fe^{i\omega t}$ reference phasor)

$$Xe^{i(\omega t+\phi)}=(Xe^{i\phi})e^{i\omega t}=(X_{\mathcal{R}e}+iX_{\mathcal{I}m})e^{i\omega t}=\mathbf{X}^{*}e^{i\omega t}$$

Complex amplitude X^{*} gives information about magnitude of X and phase relative to the force phasor

Figure 7.57 Complex amplitude $\boldsymbol{X^{*}}$.

Example: SDOF model with viscous damping

Consider the SDOF model of Figure 7.12 with viscous damping. As before, we begin with a force balance on the mass:

$$\Sigma(\text{forces acting on m}) = m\frac{d^2x(t)}{dt^2}$$

$$f(t) + kx(t) + C\frac{dx(t)}{dt} = m\frac{d^2x(t)}{dt^2}$$

But now we let the force and displacement be represented by phasors:

$$let\ f(t) = Xe^{j\omega t},\ x(t) = Xe^{j\omega t},\ \text{then}\ \frac{d^2x(t)}{dt^2} = -X\omega^2e^{j\omega t}$$

$$Fe^{j\omega t} = kXe^{j\omega t} + CXi\omega e^{j\omega t} - mX\omega^2e^{j\omega t}$$

$$F = kX + CXi\omega - m\omega^2X$$

$$\frac{X}{F} = \frac{1}{k + Ci\omega - m\omega^2} = \frac{k - m\omega^2 - Ci\omega}{\left(k - m\omega^2\right)^2 + \left(C\omega\right)^2}$$

$$\frac{X}{F} = \frac{\frac{1}{k}\left[1 - \left(\frac{\omega}{\omega_n}\right)^2 - \frac{Ci}{k}\omega\right]}{\left(1 - \left(\frac{\omega}{\omega_n}\right)^2\right)^2 + \left(\frac{C}{k}\omega\right)^2}$$

$$\frac{X}{F} = \frac{\frac{1}{k}\left[1 - \left(\frac{\omega}{\omega_n}\right)^2 - \frac{Ci}{\sqrt{km}}\omega\sqrt{\frac{m}{k}}\right]}{\left(1 - \left(\frac{\omega}{\omega_n}\right)^2\right)^2 + \left(\frac{C}{\sqrt{km}}\omega\sqrt{\frac{m}{k}}\right)^2}$$

$$\frac{X}{F} = \frac{\frac{1}{k}\left[1 - \left(\frac{\omega}{\omega_n}\right)^2 - 2\zeta i\frac{\omega}{\omega_n}\right]}{\left(1 - \left(\frac{\omega}{\omega_n}\right)^2\right)^2 + \left(2\zeta\frac{\omega}{\omega_n}\right)^2} \tag{7.48}$$

Note that we can immediately go from the differential equation of motion to an algebraic expression in the frequency domain by making the following substitutions:

$$x(t) \rightarrow X,\ \frac{dx(t)}{dt} \rightarrow i\omega X,\ \frac{d^2x(t)}{dt^2} \rightarrow \left(i\omega\right)^2X = -\omega^2X,\ f(t) \rightarrow F$$

The substitution results in the following for the viscously damped SDOF system above:

$$f(t)+kx(t)+C\frac{dx(t)}{dt}=m\frac{d^2x(t)}{dt^2}\rightarrow F+kX+CXi\omega=-m\omega^2X$$

Solving this algebraic equation results in a complex expression for the transfer function, *(X/F)*, Equation 7.48, in which the phasor angle represents the phase angle of displacement relative to the force. Often, we are only interested in the magnitude of this complex number.

Example: SDOF model with structural damping

In Equation 7.4, we substitute for k the complex value $k^*=k+i\eta k$. This expression includes the imaginary component, $i\eta k$, representing the structural damping force which is in phase with velocity but proportional to displacement.

$$F=(k+\eta ki)X-m\omega^2X$$

$$\frac{X}{F}=\frac{1}{k+\eta ki-m\omega^2}=\frac{k-m\omega^2-k\eta i}{\left(k-m\omega^2\right)^2+\left(k\eta\right)^2}$$

$$\frac{X}{F}=\frac{\frac{1}{k}\left[1-\left(\frac{\omega}{\omega_n}\right)^2-\eta i\right]}{\left(1-\left(\frac{\omega}{\omega_n}\right)^2\right)^2+\left(\eta\right)^2} \tag{7.49}$$

$$\left|\frac{X}{F}\right|=\frac{1/k}{\sqrt{\left(1-\left(\frac{\omega}{\omega_n}\right)^2\right)^2+\left(\eta\right)^2}}$$

7.10 Note on Mechanical Impedance Technique

The use of complex variables to describe mechanical vibration offers a very useful tool in developing models of more complex vibratory systems. The mechanical impedance technique is based on an analogy with alternating current electrical circuits [19]. The impedance of an electrical element is defined as the voltage amplitude, E, measured across the element divided by the current amplitude, I, flowing through the element:

$$Z=\frac{E}{I} \tag{7.50}$$

For example, the impedance for a resistor is $Z=R=E/I$. To analyze electrical networks, we apply *loop equations* (the voltage around any closed loop is zero), and *node equations* (the sum of current into any node is zero). Applying these equations allow the prediction of the current through and voltage drop across any element.

Note that the impedance in an electrical element is the voltage difference measured *across* the element, divided by the current flowing *through* the element. For an analogous mechanical element, the *across variable* is the deflection across the element (we could equivalently use velocity or acceleration) divided by the force flowing *through* the element. Note that this analogy maintains the validity of both node equations—forces sum to zero at a point, and loop equations—relative deflections around a closed path sum to zero. This electrical-mechanical analogy is summarized in Figure 7.58.

Impedance in an electrical network	Mechanical Impedance analogy
E (voltage) is measured <u>across</u> an element	X displacement (we could alternatively take velocity or acceleration as the across variable)
I (current) flows <u>through</u> an element	F Force
Impedance definition $Z\equiv$ (across variable)/(through variable) $Z=E/I$ *e.g. resistor* $E=IR$ $R=E/I$ *(impedance of a resistor, $Z=R$)*	**Impedance definition** $Z\equiv$ (across variable)/(through variable) $Z=X/F$ $Z_K=1/k$ *(spring)* $Z_M=1/(-w^2m)$ *(mass)* $Z_D=1/(i\eta k)$ *(structural damping)*
Note: •at a node, currents must sum to zero •around a closed loop, the net voltage drop is zero	**Note:** •at a point, forces must sum to zero •around a closed loop the relative displacements sum to zero

Figure 7.58 Mechanical impedance analogy.

The impedance of a general mechanical system element is:

$$Z=\frac{X}{F} \tag{7.51}$$

Table 7.8 provides the impedance for common mechanical elements.

Table 7.8 Impedance of mechanical elements.

Linear elastic stiffness element	Mass element	Viscous damping element	Stiffness element with structural damping
$Z_K=\frac{1}{k}$	$Z_M=\frac{1}{-m\omega^2}$	$Z_D=\frac{1}{i\omega C}$	$Z_K=\frac{1}{k+i\eta k}$

To solve a mechanical network, we apply node and loop equations to determine deflections and forces just as we would with an electrical network. We can also use standard impedance rules for solving electrical circuits to arrive at a result. Two important rules are:

1. For two elements, Z_1, Z_2, in series, the equivalent impedance is

$$Z_{EQ} = \frac{Z_1 Z_2}{Z_1 + Z_2} \tag{7.52}$$

2. For two elements in parallel, the equivalent impedance is

$$Z_{EQ} = Z_1 + Z_2 \tag{7.53}$$

Example: Impedance approach

As an example of this technique, consider the suspension link with identical bushings at each end, Figure 7.48. The impedance diagram for this system is shown in Figure 7.59. Note that one terminal of a mass element is always connected to an inertial reference—ground. In this example, we are interested in finding the driving point impedance: $Z_{11} = X_1/F_1$.

Elements Z_2 and Z_3 are in parallel with equivalent impedance:

$$Z_{EQ} = \frac{Z_2 Z_3}{Z_2 + Z_3}$$

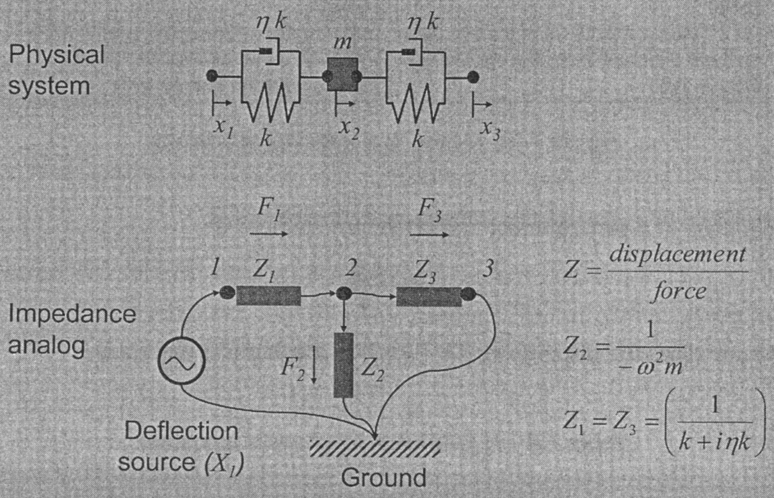

Figure 7.59 Mechanical impedance model of suspension link.

Element Z_1 is in series with this combined impedance:

$$Z_{11} = Z_1 + \left(\frac{Z_2 Z_3}{Z_2 + Z_3}\right)$$

Substituting the variables: $Z_2 = \frac{1}{-m\omega^2}$, and $Z_1 = Z_3 = \frac{1}{k + i\eta k}$ gives:

$$Z_{11} = \left(\frac{1}{k + i\eta k}\right) + \left(\frac{\left(\frac{1}{-m\omega^2}\right)\left(\frac{1}{k + i\eta k}\right)}{\left(\frac{1}{-m\omega^2}\right) + \left(\frac{1}{k + i\eta k}\right)}\right)$$

which can be simplified to:

$$|Z_{11}| = \left(\frac{2\sqrt{\left(1 - \left(\frac{\omega}{\omega_2}\right)^2\right)^2 + (\eta)^2}}{k\sqrt{1 + (\eta)^2}\sqrt{\left(1 - \left(\frac{\omega}{\omega_1}\right)^2\right)^2 + (\eta)^2}}\right)$$

$$\omega_1 = \sqrt{\frac{k}{m}}$$

$$\omega_2 = \sqrt{\frac{2k}{m}}$$

References

1. Thomson, W., *Vibration Theory and Applications*, Prentice-Hall, NJ, 1965.
2. Gillespie, T. D., *Fundamentals of Vehicle Dynamics*, SAE International, Warrendale, PA, 1992, p. 465.
3. Lee, R. and Pradko, F., "Analytical Analysis of Human Vibration," SAE Paper No. 68001, SAE International, Warrendale, PA, 1968.
4. Stikeleather, L., Hall, G. and Radke, A., "A Study of Vehicle Vibration Spectra as Related to Seating Dynamics," SAE Paper No. 720001, SAE International, Warrendale, PA, 1972.
5. Kamal M. and Wolf, J., *Modern Automotive Structural Analysis*, Van Nostrand Reinhold, NY, 1982, p. 55.
6. Meirovitch, L., *Elements of Vibration Analysis*, McGraw Hill, NY, 1986, pp. 45–72.
7. Malen, D. E., *Applied Damping in the Automobile Body*, Masters Thesis, Massachusetts Institute of Technology, MA, 1970.

8. Flugge, W., *Viscoelasticity*, Blaisdell Publishing, MA, 1967, p. 54.
9. Den-Hartog, J., *Mechanical Vibrations*, McGraw Hill, NY, 1956, Chapter 5.
10. Gillespie, T. D., *Fundamentals of Vehicle Dynamics*, SAE International, Warrendale, PA, 1992, pp. 129–147.
11. Kikuchi, N. and Malen, D., *Course notes for ME513 Fundamentals of Body Engineering*, University of Michigan, Ann Arbor, MI, 2007.
12. Elliott, W., "Plastic Models for Dynamic Structural Analysis, SAE Paper No. 710262, SAE International, Warrendale, PA, 1971.
13. Lyon, R., *Machinery Noise and Diagnostics*, Butterworths, MA, 1987.
14. Davis, J., "Modal Modeling Techniques for Vehicle Shake Analysis," SAE Paper No. 720045 SAE International, Warrendale, PA, 1972.
15. Kato, T., Hoshi, K. and Umemura, E., "Application of Soap Film Geometry for Low Noise Floor Panels," *Proceedings of the 1999 Noise and Vibration Conference*, P-342, SAE 1999-01-1799, SAE International, Warrendale, PA, 1999. Also "Harrier/Lexus RX300 Uniform-curvature panels to isolate road noise," *Automotive Engineering International*, SAE International, Warrendale, PA, April, 1998, p24.
16. Snowdon, J. C., *Vibration and Shock in Damped Mechanical Systems*, John Wiley, NY, 1968, Chapter 5.
17. Cogswell, J. and Malen, D., E., "Engine Mount for Integral Body Vehicle," SAE Paper No. 830258, SAE International, Warrendale, PA, 1983.
18. Kennedy, C. and Pancu, C., "Use of Vectors in Vibration Measurement and Analysis," *Journal of the Aeronautical Sciences*, V14, N11, November, 1947.
19. Shearer, J., Murpy, A., and Richardson, H., *Introduction to System Dynamics*, Addison-Wesley, MA, 1967.